

Commensurate-incommensurate transitions of quantum Hall stripe states in double-quantum-well systems

R. Côté,¹ H. A. Fertig,² J. Bourassa,¹ and D. Bouchiat¹

¹Département de physique and CERPEMA, Université de Sherbrooke, Sherbrooke, Québec, Canada, J1K 2R1

²Department of Physics and Astronomy, University of Kentucky, Lexington KY 40506-0055

(Dated: February 1, 2008)

In higher Landau levels ($N > 0$) and around filling factors $\nu = 4N + 1$, a two-dimensional electron gas in a double-quantum-well system supports a stripe groundstate in which the electron density in each well is spatially modulated. When a parallel magnetic field is added in the plane of the wells, tunneling between the wells acts as a spatially rotating effective Zeeman field coupled to the “pseudospins” describing the well index of the electron states. For small parallel fields, these pseudospins follow this rotation, but at larger fields they do not, and a commensurate-incommensurate transition results. Working in the Hartree-Fock approximation, we show that the combination of stripes and commensuration in this system leads to a very rich phase diagram. The parallel magnetic field is responsible for oscillations in the tunneling matrix element that induce a complex sequence of transitions between commensurate and incommensurate liquid or stripe states. The homogeneous and stripe states we find can be distinguished by their collective excitations and tunneling $I - V$, which we compute within the time-dependent Hartree-Fock approximation.

PACS numbers: 73.43.-f, 73.21.-b

I. INTRODUCTION

In strong magnetic fields, the two-dimensional electron gas (2DEG) in a double quantum well system (DQWS) is well known to support spontaneous interlayer coherence if the interwell separation is smaller than some critical value d_c . At filling factor $\nu = 1$, the interlayer coherence is responsible for many interesting properties of the 2DEG such as a quantum Hall state, a Goldstone mode¹ (in the absence of tunneling) associated with the broken U(1) symmetry of the pseudospin order in the ground state, which has been recently detected experimentally², and exotic topological quasiparticle excitations such as merons and bimerons. When the magnetic field is inclined towards the plane of the 2DEG in the $\nu = 1$ coherent state, a radical change in the behavior of the transport gap was observed³ and explained as a commensurate-incommensurate transition in the pseudospin order⁴. A review of these properties can be found in Ref. 5.

At bigger filling factors, in Landau levels $N > 0$, it has been shown⁶ that the 2DEG in a DQWS can support states where both the electronic densities and the interlayer coherence are spatially modulated. Ref. 6 discussed the ground state of the DQWS at filling factors $\nu = 4N + 1$ when both wells have exactly the same number of electrons using the Hartree-Fock approximation. They showed that, for some range of interwell separations, a “staggered” stripe state is lowest in energy. This state involves a unidirectional charge density wave ordering of electrons in each well, such that the regions of high electron density in one well are nearest to regions of low electron density in the other. Stripe states in single well systems were first discussed by Koulakov, Fogler, and Shklovskii and Moessner and Chalker⁷ and are believed to explain a large anisotropy observed in transport experiments for quantum Hall systems in moderate magnetic fields, for which the highest energy occupied Landau level is approximately half-filled⁸.

In a DQWS, stripe states are more complex and interesting than in the single layer case because of the possibility that interlayer coherence may coexist with charge ordering. In the staggered stripe state, interlayer coherence is maintained only along linear regions at the edges of the stripes. These “linear coherent regions” (LCR’s), whose width decreases with increasing interlayer separation, support topological quasiparticle excitations closely akin to sine-Gordon solitons⁶. In the absence of tunneling, Côté and Fertig⁹ showed that this staggered stripe state supports two Goldstone modes associated respectively with broken translational symmetry and broken U(1) symmetry associated with interlayer coherence.

In this paper, we address the questions of how the staggered stripe state and its collective excitations are modified by the presence of a magnetic field component parallel to the plane of the layers and how these changes are reflected in the tunneling current. We recall⁵ that, in the presence of a parallel magnetic field, the tunneling hamiltonian can be written as an effective Zeeman coupling of the form

$$H_T = - \int d\mathbf{r} \mathbf{h}(\mathbf{r}) \cdot \mathbf{S}(\mathbf{r}), \quad (1)$$

where $\mathbf{S}(\mathbf{r})$ is the pseudospin density and $\mathbf{h}(\mathbf{r})$ is a pseudo-magnetic field that rotates in the xy plane. In this paper,

we choose \mathbf{B}_\parallel along the y axis and use a gauge in which this pseudo-field is given by

$$\mathbf{h}(\mathbf{r}) = 2t_N(Q) [\cos(Qx)\hat{\mathbf{x}} - \sin(Qx)\hat{\mathbf{y}}], \quad (2)$$

where $Q = d/\ell_\parallel^2$, with d the separation between the wells, and $\ell_\parallel = \sqrt{\hbar c/eB_\parallel}$ the magnetic length due to the in-plane component B_\parallel of the magnetic field. At filling factor $\nu = 1$, the ground state at small layer separation and $B_\parallel = 0$ is well approximated by a state in which all pseudospins are oriented along the x axis (we assume that the bare tunneling energy t_0 is not zero). When the parallel magnetic field is turned on, the pseudospins rotate in the xy plane, aligning with the local orientation of $\mathbf{h}(\mathbf{r})$. This defines a uniform commensurate state, which we will call the commensurate liquid (CL). When B_\parallel increases, the rotation period of the pseudospins decreases. This rotation is opposed by the Coulomb exchange interaction that tends to keep pseudospins parallel. Above some critical B_\parallel , there is a phase transition to an incommensurate state where the pseudospins no longer rotate with the in-plane field but instead tend to align along some common direction as B_\parallel increases above the critical value. We call this state the incommensurate liquid (IL) state. It is this change in the ground state of the 2DEG with B_\parallel that is believed to be responsible for the radical change in the behavior of the transport gap observed by Murphy *et al.*³

In the experiment of Murphy *et al.*, the system consisted of two homogeneous two-dimensional electron gas (2DEG) with filling factor (in each well) $\tilde{\nu} = 1/2$ and in Landau level $N = 0$. The same commensurate-incommensurate transition should occur in higher Landau levels at total filling factors $\nu = 4N + 1$. In this case, however, we must recognize that, for $d > d_c(N)$, the system is unstable to the formation of stripes as was shown in Ref. 9. In the pseudospin language, this staggered stripe state consists of pseudospin modulation in the xz plane. Applying a parallel magnetic field will tend to induce a commensurate rotation of the pseudospins in the xy plane in addition to the xz modulations. In this paper, we call this phase a commensurate stripe phase (CSP). If the parallel field is too strong, the exchange energy cost of this commensurate rotation will be prohibitive and the ground state will revert to a state with xz modulations only as if there were no tunneling and no parallel field. We call this other state an incommensurate stripe phase (ISP). As d and B_\parallel are changed for a given tunneling parameter, we thus expect a rich phase diagram with transitions between the four possible states just introduced: CL, IL, CSP and ISP. (We cannot, of course, rule out the possibility of other ground states with lower energy).

In higher Landau levels, the effect of B_\parallel is more complex than for $N = 0$. This is because the tunneling amplitude in the N th Landau level has a non trivial B_\parallel dependence, $t_N(Q) = t_0 e^{-Q^2 \ell_\perp^2/4} L_N^0 \left(\frac{Q^2 \ell_\perp^2}{2} \right)$, with t_0 the bare tunneling amplitude. For $N > 0$, this tunneling amplitude oscillates with wavevector $Q = d/\ell_\parallel^2$, becoming negative in some range of B_\parallel . One effect of these oscillations is that B_\parallel can induce not only one but several (reentrant) commensurate-incommensurate transitions in the liquid or in the stripe phases depending on the value of N . Figure 1 illustrates some typical phase diagrams we find for several values of the bare tunneling parameter t_0 . These figures will be explained in more detail below.

Another effect of the parallel field is that, in the commensurate stripe phase (CSP), the long-wavelength dispersion relations of the low-energy phonon and pseudospin wave modes will be strongly dependent on B_\parallel through $t_N(Q)$. We find that the gap in the pseudospin wave mode (which is related to the broken U(1) symmetry of the pseudospin order) and in the phonon mode (at finite wavevector) follows the oscillations of the tunneling amplitude $t_N(Q)$. In particular, the phonon and pseudospin wave modes become essentially gapless whenever the parallel field is such that $t_N(Q)$ is close to one of its N zeroes. Such behavior is not seen in the incommensurate stripe phase (ISP) since the properties of this state are independent of $t_N(Q)$ and so of B_\parallel . We thus find that the CSP and ISP are clearly distinguishable by their low-energy collective modes. Figure 2 illustrates these modes as computed using the time-dependent Hartree-Fock approximation, as explained in more detail below.

One way to probe these states is via interlayer tunneling. For very small values of t_0 , the tunneling $I - V$ has been argued¹⁰ and shown² to probe the Goldstone mode dispersion of the (spontaneously) coherent state as the parallel field is adjusted. An analogous effect occurs in the stripe state of this system, as illustrated in Fig. 3. A clear signature of the existence of stripes can be found by noting the non-monotonic behavior of the tunneling peak as a function of B_\parallel . In particular, one finds this peak at zero bias voltage for $B_\parallel = nhc/ade$ where a is the separation between the stripes in a given well and $n = 0, 1, 2, \dots$. This is a reflection of the periodicity of the collective mode spectrum illustrated in Fig. 2(a), and directly demonstrates the existence of stripes in the groundstate.

This paper is organized as follows. In Sec. II, we derive the tunneling Hamiltonian in the presence of the parallel magnetic field and explain the origin of the oscillations in $t_N(Q)$. In Sec. III, we derive the Hartree-Fock equations of motion for the single-particle Green's function from which we compute the density and pseudospin density as well as the energy of the commensurate and incommensurate stripe states. The energy of these phases are compared with those of the commensurate and incommensurate liquid phases in Sec. IV to obtain the phase diagram, in Landau level $N = 2$, for various parameters B_\parallel, t_0 , and d . We briefly review, in Sec. V, the formalism necessary to compute the susceptibilities and dispersion relations in the time-dependent Hartree-Fock approximation (TDHFA) and present

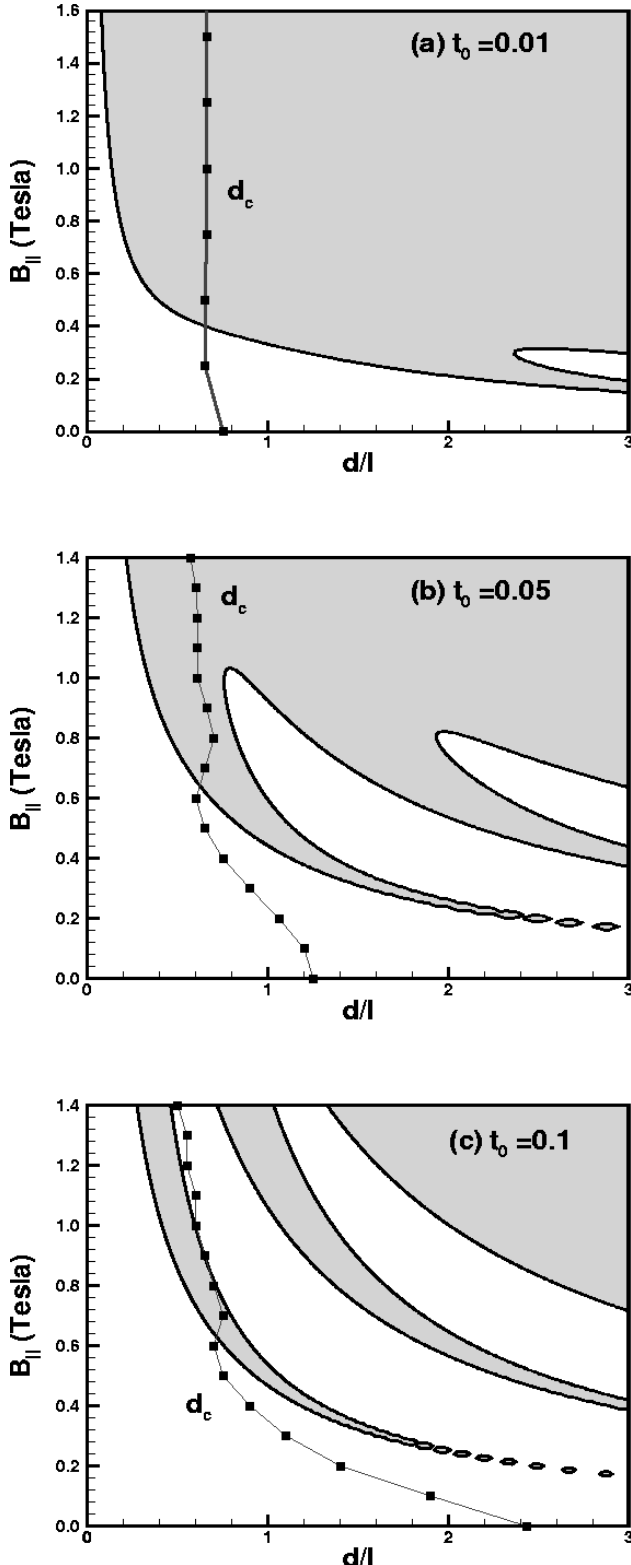


FIG. 1: Phase diagram of the 2DEG in Landau level $N = 2$ in the $B_{\parallel} - d/\ell_{\perp}$ plane for values of the bare tunneling parameters equal to (a) $t_0/(e^2/\kappa\ell) = 0.01$, (b) $t_0/(e^2/\kappa\ell) = 0.05$ and (c) $t_0/(e^2/\kappa\ell) = 0.1$. The areas in white(gray) represent the commensurate(incommensurate) liquid state. The heavy line marked d_c indicates the critical spacing above which one of the stripe state (either commensurate or incommensurate) is lower in energy than both the CL and IL phases.

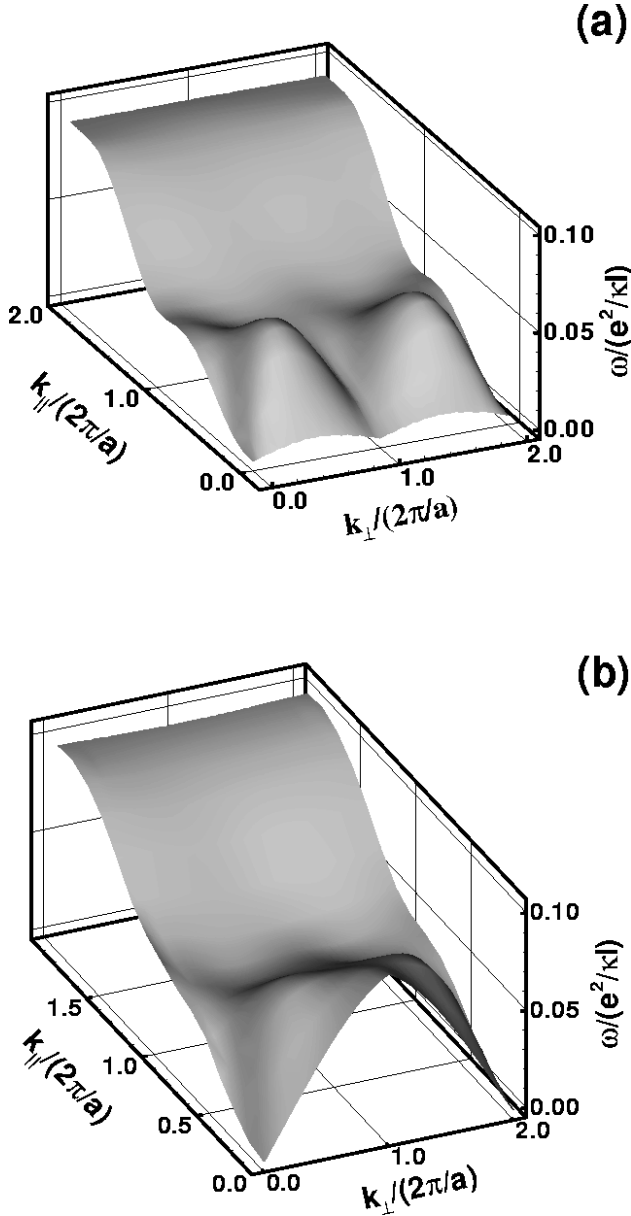


FIG. 2: Dispersion relations of the low-energy modes in (a) the ISP and (b) the CSP for $N = 2$, $t_0/(e^2/\kappa\ell) = 0.01$ and $B_{\parallel} = 0$ T.

our numerical results in various region of the phase diagram studied in Sec. IV. Section VI shows how the tunneling current, in the stripe states, is affected by the parallel magnetic field. We conclude in Sec. VII.

II. TUNNELING HAMILTONIAN

We consider an unbiased symmetric DQWS in a tilted magnetic field $\mathbf{B} = B_{\parallel}\hat{\mathbf{y}} + B_{\perp}\hat{\mathbf{z}}$ at total filling factor $\nu = 4N + 1$ where $N = 0, 1, 2, \dots$ is the Landau level index. To simplify the analysis, we make several approximations. We retain only one electric subband of the DQWS, and assume that $g^*\mu_B B \gg \Delta_{SAS}$ where Δ_{SAS} is the symmetric to antisymmetric gap so that the real spins are completely frozen. Furthermore, we consider the lower Landau levels as filled and inert and neglect any Landau level mixing. Considering very narrow wells and treating the tunneling term in a tight-binding approximation, the non-interacting Hamiltonian of the 2DEG can be written, in the gauge

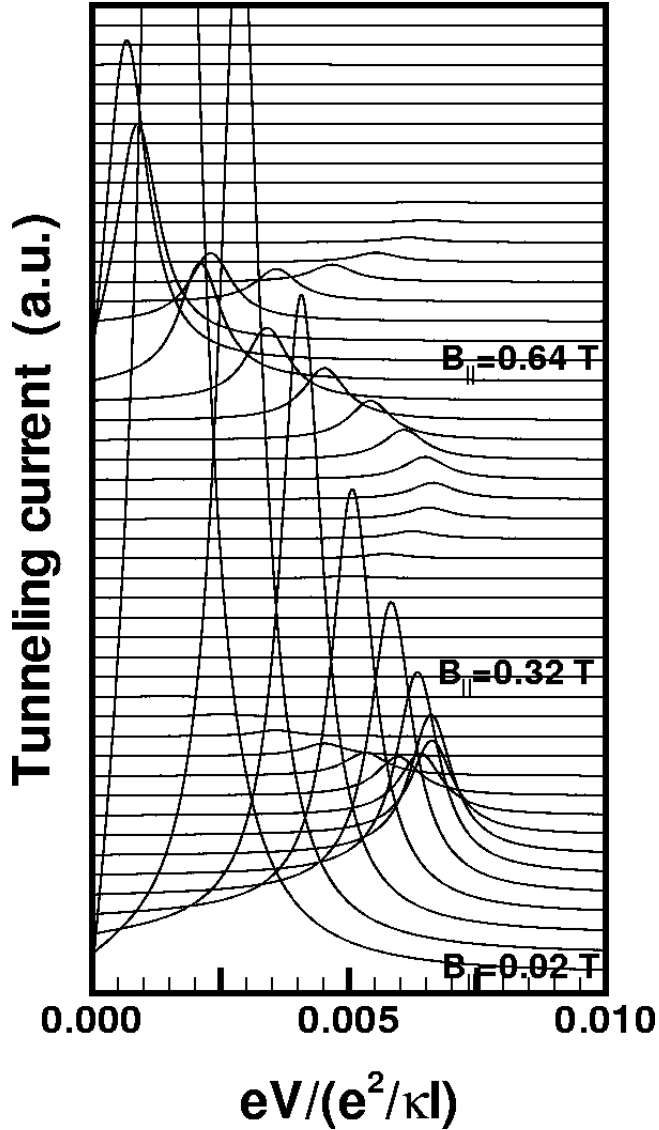


FIG. 3: Variation of the tunneling current $I(t)$ with the potential bias eV for several values of the parallel magnetic field in the CSP. The tunneling current is calculated by using the first term in Eq. (81) and with $N = 2, t_0/(e^2/\kappa\ell) = 0.01$ and $d/\ell_\perp = 1.4$. Note that $B_\parallel = 0.325$ T corresponds approximately to $Q\ell_\perp = 2\pi/a$ where a is the separation between the stripes in a given well.

where $\mathbf{A} = (0, B_\perp x, -B_\parallel x)$, as

$$H_0 = \sum_{X,j} E_0 c_{X,j}^\dagger c_{X,j} - \sum_X t_N(Q) \left(e^{iQX} c_{X,R}^\dagger c_{X,L} + e^{-iQX} c_{X,L}^\dagger c_{X,R} \right), \quad (3)$$

where E_0 is the electron energy in each isolated well and $c_{\alpha,X}^\dagger$ is the creation operator for an electron in Landau level N , guiding center index X , and well index $j = R, L$. The electronic wavefunctions are given by

$$\psi_{N,X,j}(\mathbf{r}) = \frac{1}{\sqrt{L_y}} e^{-iXy/\ell^2} \varphi_N(x - X) \chi_j(z), \quad (4)$$

where $\chi_j(z)$ is the envelope wave function of the lowest-energy electric subband centered on the right or left well and $\varphi_N(x)$ is an eigenfunction of the one-dimensional harmonic oscillator. In the tight-binding approximation, the

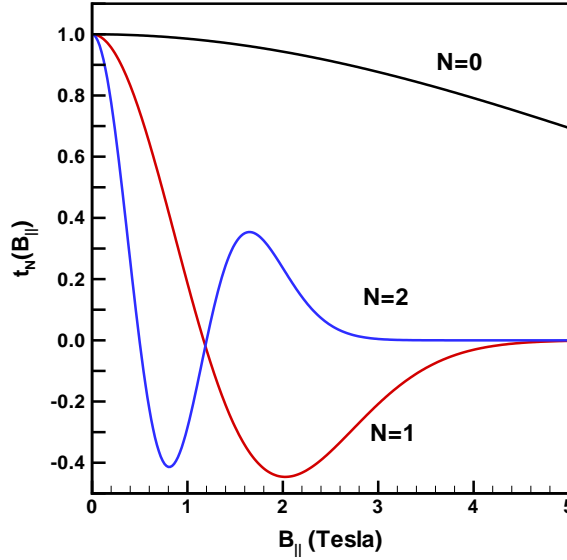


FIG. 4: Variation of the tunneling amplitude $t_N(Q)$ with the parallel magnetic field for filling fractions $\nu = 1, 5, 9$ corresponding to Landau levels $N = 0, 1, 2$ and for $d/\ell_{\perp} = 1.0$.

tunneling amplitude, $t_N(Q)$, is given by

$$t_N(Q) = -t_0 \int_{-\infty}^{+\infty} dx \varphi_N(x - X) e^{iQx} \varphi_N(x - X) = t_0 e^{-Q^2 \ell_{\perp}^2 / 4} L_N^0 \left(\frac{Q^2 \ell_{\perp}^2}{2} \right), \quad (5)$$

where t_0 is the bare tunneling amplitude (defined as a positive quantity), $L_N^0(x)$ is a generalized Laguerre's polynomial and the wavevector and $Q = d/\ell_{\perp}^2$ where $\ell_{\perp} = \sqrt{\hbar c/eB_{\perp}}$ is the magnetic length associated with the parallel magnetic field.

If $N > 0$, the tunneling amplitude oscillates with the strength of the parallel field and/or the separation between the wells¹¹. (In this paper, we neglect the further dependency of t_0 on d due to the change in the overlap of the electric subband wavefunctions $\chi_j(z)$ of the two wells). We remark that the first zero of $t_N(Q)$ appears at relatively small parallel field. For example, since $2\pi n_0 \ell_{\perp}^2 = \nu$ where n_0 is the total areal density of the electrons in the DQWS, the wavevector $Q\ell_{\perp} = \nu(d/\ell_{\perp})(e/n_0 hc) B_{\parallel}$, and so $d/\ell_{\perp} = d\sqrt{2\pi n_0/\nu}$. If we assume a typical total electronic density of $n_0 = 1 \times 10^{11} \text{ cm}^{-2}$, we have, with B_{\parallel} in Tesla, $Q\ell_{\perp} = 0.242(\nu)(d/\ell_{\perp}) B_{\parallel}$. On the other hand, at this density the separation between the wells can be expressed as $(d/\ell_{\perp}) = 0.793d(100\text{\AA})/\sqrt{\nu}$. For total filling factor $\nu = 1$, we get $d/\ell_{\perp} = 1.6$ for a typical interwell separation of 200 Å. This value decreases as N increases at fixed total density. Figure 4 shows the behavior of $t_N(Q)$ for $d/\ell_{\perp} = 1.0$, $n_0 = 1 \times 10^{11} \text{ cm}^{-2}$ and filling fractions $\nu = 1, 5, 9$ corresponding to $N = 0, 1, 2$. We see from this figure that for $N = 2$, $t_N(Q)$ vanishes near $B_{\parallel} \approx 0.5 \text{ T}$ and 1.2 T , and that a parallel field of $\approx 3 \text{ T}$ is required to reach the asymptotic behavior of the tunneling amplitude.

III. HARTREE-FOCK EQUATIONS OF MOTION

We describe the various ordered coherent states of the electrons in the partially filled Landau level N by the set of average values $\{\langle \rho_{i,j}(\mathbf{q}) \rangle\}$ where $\rho_{i,j}(\mathbf{q})$ is an operator that we define¹² by

$$\rho_{i,j}(\mathbf{q}) = \frac{1}{N_{\varphi}} \sum_X e^{-iq_x X + iq_x q_y \ell^2 / 2} c_{i,X}^{\dagger} c_{j,X - q_y \ell^2}, \quad (6)$$

where N_{φ} is the Landau level degeneracy. At a semiclassical level, the $\langle \rho_{i,i}(\mathbf{q}) \rangle'$ s can be thought of as the Fourier transform of the density of guiding centers of the cyclotron orbits while the off diagonal terms $\langle \rho_{i \neq j}(\mathbf{q}) \rangle$ describe

quantum coherence between the two 2DEG. The average values $\langle \rho_{i,j}(\mathbf{q}) \rangle$ are obtained by computing the single-particle Green's function

$$G_{i,j}(X, X', \tau) = -\left\langle T c_{i,X}(\tau) c_{j,X'}^\dagger(0) \right\rangle, \quad (7)$$

whose Fourier transform we define as

$$G_{i,j}(\mathbf{q}, \tau) = \frac{1}{N_\phi} \sum_{X, X'} e^{-\frac{i}{2}q_x(X+X')} \delta_{X, X' - q_y l^2} G_{i,j}(X, X', \tau), \quad (8)$$

so that $G_{i,j}(\mathbf{q}, \tau = 0^-) = \langle \rho_{j,i}(\mathbf{q}) \rangle$.

Using the tunneling Hamiltonian H_0 [Eq. (3)] and working in the Hartree-Fock approximation, we find that the single-particle Green's functions for the DQWS obey the system of equations

$$\begin{aligned} & [i\hbar\omega_n - (E_0 - \mu)] G_{R,R}(\mathbf{q}, \omega_n) + t^*(\mathbf{q}) G_{L,R}(\mathbf{q} - \mathbf{Q}, \omega_n) \\ & - \sum_{\mathbf{q}'} U_{R,R}(\mathbf{q}, \mathbf{q}') G_{R,R}(\mathbf{q}', \omega_n) - \sum_{\mathbf{q}'} U_{R,L}(\mathbf{q}, \mathbf{q}') G_{L,R}(\mathbf{q}', \omega_n) = \hbar\delta_{\mathbf{q},0}, \end{aligned} \quad (9)$$

$$\begin{aligned} & [i\hbar\omega_n - (E_0 - \mu)] G_{R,L}(\mathbf{q}, \omega_n) + t^*(\mathbf{q}) G_{L,L}(\mathbf{q} - \mathbf{Q}, \omega_n) \\ & - \sum_{\mathbf{q}'} U_{R,R}(\mathbf{q}, \mathbf{q}') G_{R,L}(\mathbf{q}', \omega_n) - \sum_{\mathbf{q}'} U_{R,L}(\mathbf{q}, \mathbf{q}') G_{L,L}(\mathbf{q}', \omega_n) = 0, \end{aligned} \quad (10)$$

$$\begin{aligned} & [i\hbar\omega_n - (E_0 - \mu)] G_{L,R}(\mathbf{q}, \omega_n) + t(\mathbf{q}) G_{R,R}(\mathbf{q} + \mathbf{Q}, \omega_n) \\ & - \sum_{\mathbf{q}'} U_{L,R}(\mathbf{q}, \mathbf{q}') G_{R,R}(\mathbf{q}', \omega_n) - \sum_{\mathbf{q}'} U_{L,L}(\mathbf{q}, \mathbf{q}') G_{L,R}(\mathbf{q}', \omega_n) = 0, \end{aligned} \quad (11)$$

$$\begin{aligned} & [i\hbar\omega_n - (E_0 - \mu)] G_{L,L}(\mathbf{q}, \omega_n) + t(\mathbf{q}) G_{R,L}(\mathbf{q} + \mathbf{Q}, \omega_n) \\ & - \sum_{\mathbf{q}'} U_{L,R}(\mathbf{q}, \mathbf{q}') G_{R,L}(\mathbf{q}', \omega_n) - \sum_{\mathbf{q}'} U_{L,L}(\mathbf{q}, \mathbf{q}') G_{L,L}(\mathbf{q}', \omega_n) = \hbar\delta_{\mathbf{q},0}. \end{aligned} \quad (12)$$

The tunneling term $t(\mathbf{q})$ is, in our particular geometry where the parallel magnetic field is along the y axis, given by

$$t(\mathbf{q}) = t_N(Q) e^{iQq_y l_\perp^2/2}. \quad (13)$$

When $Q = 0$, Eqs. (9)-(12) is the system of equations we studied in Ref. 9. The Coulomb interactions and averaged densities in this system of equations produce the mean field potentials

$$\begin{aligned} U_{R,R}(\mathbf{q}, \mathbf{q}') &= \left(\frac{e^2}{\kappa l_\perp} \right) [H(\mathbf{q} - \mathbf{q}') - X(\mathbf{q} - \mathbf{q}')] \langle \rho_{R,R}(\mathbf{q} - \mathbf{q}') \rangle \gamma_{\mathbf{q}, \mathbf{q}'} + \left(\frac{e^2}{\kappa l_\perp} \right) \tilde{H}(\mathbf{q} - \mathbf{q}') \langle \rho_{L,L}(\mathbf{q} - \mathbf{q}') \rangle \gamma_{\mathbf{q}, \mathbf{q}'}, \\ U_{L,L}(\mathbf{q}, \mathbf{q}') &= \left(\frac{e^2}{\kappa l_\perp} \right) [H(\mathbf{q} - \mathbf{q}') - X(\mathbf{q} - \mathbf{q}')] \langle \rho_{L,L}(\mathbf{q} - \mathbf{q}') \rangle \gamma_{\mathbf{q}, \mathbf{q}'} + \left(\frac{e^2}{\kappa l_\perp} \right) \tilde{H}(\mathbf{q} - \mathbf{q}') \langle \rho_{R,R}(\mathbf{q} - \mathbf{q}') \rangle \gamma_{\mathbf{q}, \mathbf{q}'}, \\ U_{R,L}(\mathbf{q}, \mathbf{q}') &= - \left(\frac{e^2}{\kappa l_\perp} \right) \tilde{X}(\mathbf{q} - \mathbf{q}') \langle \rho_{L,R}(\mathbf{q} - \mathbf{q}') \rangle \gamma_{\mathbf{q}, \mathbf{q}'}, \end{aligned} \quad (14)$$

$$U_{L,R}(\mathbf{q}, \mathbf{q}') = - \left(\frac{e^2}{\kappa l_\perp} \right) \tilde{X}(\mathbf{q} - \mathbf{q}') \langle \rho_{R,L}(\mathbf{q} - \mathbf{q}') \rangle \gamma_{\mathbf{q}, \mathbf{q}'}, \quad (15)$$

where

$$\gamma_{\mathbf{q}, \mathbf{q}'} = e^{-i(\mathbf{q} \times \mathbf{q}') \cdot \hat{\mathbf{z}} l_\perp^2/2}. \quad (16)$$

The definitions of the coulomb interactions H , X , \tilde{H} and \tilde{X} were given in Ref. 9. They are respectively the Fourier transforms of the intrawell Hartree and Fock interactions and the interwell Hartree and Fock interactions.

Once the densities are extracted from the single-particle Green's functions, the Hartree-Fock energy per electron can be written as

$$\begin{aligned} \frac{E_{HF}}{N_e} = & -\frac{2}{\nu} t_N(Q) \operatorname{Re} [\langle \rho_{R,L}(\mathbf{Q}) \rangle] \\ & + \frac{1}{2\nu} \left(\frac{e^2}{\kappa l_\perp} \right) \sum_{\mathbf{q} \neq 0} H(\mathbf{q}) \left[|\langle \rho_{R,R}(\mathbf{q}) \rangle|^2 + |\langle \rho_{L,L}(\mathbf{q}) \rangle|^2 \right] \\ & - \frac{1}{2\nu} \left(\frac{e^2}{\kappa l_\perp} \right) \sum_{\mathbf{q}} X(\mathbf{q}) \left[|\langle \rho_{R,R}(\mathbf{q}) \rangle|^2 + |\langle \rho_{L,L}(\mathbf{q}) \rangle|^2 \right] \\ & + \frac{1}{\nu} \left(\frac{e^2}{\kappa l_\perp} \right) \sum_{\mathbf{q} \neq 0} \tilde{H}(\mathbf{q}) [\langle \rho_{R,R}(-\mathbf{q}) \rangle \langle \rho_{L,L}(\mathbf{q}) \rangle] \\ & - \frac{1}{\nu} \left(\frac{e^2}{\kappa l_\perp} \right) \sum_{\mathbf{q}} \tilde{X}(\mathbf{q}) |\langle \rho_{L,R}(\mathbf{q}) \rangle|^2. \end{aligned} \quad (17)$$

The $\langle \rho_{i,j}(\mathbf{q}) \rangle'$'s are found by solving Eqs. (10)-(13), and using Eqs. (7)-(9) to extract them from the resulting Green's functions. Since the potentials entering the former set of equations involve the $\langle \rho_{i,j}(\mathbf{q}) \rangle'$'s, this procedure must be iterated until convergence is achieved. (The numerical scheme is described in more detail in Ref. 12.) We next describe the results of such calculations for several possible states, and discuss the phase diagram of the system.

IV. NON-HOMOGENEOUS HARTREE-FOCK STATES IN HIGHER LANDAU LEVELS

In Refs. 6 and 9, it was found, for $B_{\parallel} = 0$, that, with the exception of the $N = 0$ Landau level, the 2DEG ground state first evolves from a uniform coherent state (UCS) to a unidirectional CDW state, and then undergoes a first order transition to a modulated stripe phase as d/ℓ_\perp is increased from zero. Wigner crystal (WC) states were found to be higher in energy than the unidirectional modulated states for $N > 0$. In the $N = 0$ Landau level, the evolution was shown to be from a uniform coherent state to a CDW state and then to a Wigner crystal state at large interwell separation. The coherent states (either CDW or WC) are always lower in energy than their incoherent counterparts.

In this paper, we consider the consequences to the stability of these unidirectionally ordered states of adding a parallel magnetic field. In view of our earlier results, we restrict ourselves to higher Landau levels $N > 0$ and consider only coherent states. (Incoherent states are insensitive to the parallel field). Our filling factor is $\nu = 4N + 1$ and we consider four possible groundstates. These states are best described in a pseudospin language where the right (left) well electronic state is associated with a pseudospin up (down) state. The $\rho_{i,j}$ operators defined above can be mapped into the density and pseudospin density operators by the relations

$$n(\mathbf{q}) = \frac{1}{2} [\rho_{R,R}(\mathbf{q}) + \rho_{L,L}(\mathbf{q})], \quad (18)$$

$$\rho_x(\mathbf{q}) = \frac{1}{2} [\rho_{R,L}(\mathbf{q}) + \rho_{L,R}(\mathbf{q})], \quad (19)$$

$$\rho_y(\mathbf{q}) = \frac{1}{2i} [\rho_{R,L}(\mathbf{q}) - \rho_{L,R}(\mathbf{q})], \quad (20)$$

$$\rho_z(\mathbf{q}) = \frac{1}{2} [\rho_{R,R}(\mathbf{q}) - \rho_{L,L}(\mathbf{q})]. \quad (21)$$

The tunneling hamiltonian of Eq. (3) can be written as an effective “Zeeman” coupling

$$H_T = - \sum_X \mathbf{h}(X) \cdot \boldsymbol{\rho}(X), \quad (22)$$

where $\boldsymbol{\rho}(X)$ and $n(X)$ are the (guiding center-) spin density and density operators respectively. The field $\mathbf{h}(X)$ plays the role of a pseudo-magnetic field that lies in the plane of the 2DEG and rotates in the space of the X coordinate according to

$$\mathbf{h}(X) = 2t_N(Q) [\cos(QX) \hat{\mathbf{x}} - \sin(QX) \hat{\mathbf{y}}], \quad (23)$$

with a period $\lambda = 2\pi/Q = 2\pi\ell_{\parallel}^2/d$. (The minus sign in Eq. (23) is due to our particular convention for associating the R and L wells with the up and down spins).

When the magnetic field is tilted towards the plane of the 2DEG (at constant B_{\perp} to keep the filling fraction constant), the rotation period λ of the pseudospins decreases. In a non-interacting picture, the pseudospins would align with the local field $\mathbf{h}(X)$ to minimize the tunneling energy. When electron-electron interactions are taken into account, however, the pseudospins interact through an effective exchange interaction⁴ that favors a parallel configuration of the pseudospins. At small parallel magnetic field, the pseudospins can follow the effective Zeeman field. The resulting state is called the commensurate liquid (CL). Above some critical parallel magnetic field, $B_{\parallel,c}$, the exchange energy cost of the rotation is too high, and an incommensurate liquid (IL) state where the pseudospins are spatially uniform becomes lower in energy. We note that this incommensurate state is never the true ground state: at a field slightly lower than $B_{\parallel,c}$, the 2DEG has a transition into a soliton lattice state (SLS) where kinks (slips of 2π in the phase of the rotating pseudospins) form a lattice in the direction perpendicular to the parallel magnetic field with a period $\lambda_s(Q)$. This SLS continuously evolves into the IL as the parallel field is increased. We do not explicitly treat the SLS in our work since it is significantly different than the IL only in a small range of Q (see, for example, Ref. 13). We will thus refer to the commensurate-incommensurate transition as to the transition between the CL and the IL.

The CL and IL states are spatially homogeneous; their orderings are characterized by the behavior of $\langle \rho_{i \neq j}(\mathbf{q}) \rangle$ but have no non-vanishing values of $\langle \rho_{ii}(\mathbf{q} \neq 0) \rangle$. In high Landau levels, stripe states may form^{6,7} which have guiding center densities oscillating spatially between the wells. It was found in Ref. 6 that for d/ℓ_{\perp} not too small, the edges of the stripes in each well will admix to form linear coherent regions (LCR's), and that in the pseudospin language such states are akin to helical ferromagnets⁹. In the presence of a parallel field, the pseudospin ordering in the LCR's may or may not follow the effective Zeeman field, leading to a commensurate stripe phase (CSP) and an incommensurate stripe phase (ISP) .

A. Commensurate Liquid (CL)

The commensurate liquid at $\nu = 1$ and with $t_N(Q) > 0$ is defined by homogeneous and equal densities of electrons in both wells and by a rotation of the pseudospins in the xy plane with a single period $\lambda = 2\pi\ell_{\parallel}^2/d$. The order parameters of this state are given by

$$\langle \rho_{R,R}(0) \rangle = \langle \rho_{L,L}(0) \rangle = \frac{1}{2}, \quad (24)$$

$$\langle \rho_{R,L}(-\mathbf{Q}) \rangle = \langle \rho_{L,R}(\mathbf{Q}) \rangle = \frac{1}{2}. \quad (25)$$

All other ρ 's vanish in this state. The energy per particle $E_{CL} = E_{HF}/N_e$ (N_e is the number of electrons in the partially filled level) is simply

$$E_{CL} = -|t_N(Q)| - \frac{1}{4} \left(\frac{e^2}{\kappa l_{\perp}} \right) [X(0) + \tilde{X}(\mathbf{Q})]. \quad (26)$$

The absolute value in Eq. (26) is necessary since, when $t_N(Q) < 0$, the pseudo-magnetic field reverses direction and we must have $\langle \rho_{R,L}(-\mathbf{Q}) \rangle = -\frac{1}{2}$.

B. Incommensurate Liquid (IC)

The incommensurate liquid is a state with equal and homogeneous densities in both wells and with the pseudospins all aligned in the same direction which we take here as the x axis. The only non-vanishing order parameters are

$$\langle \rho_{R,L}(0) \rangle, \langle \rho_{L,R}(0) \rangle = \frac{1}{2}, \quad (27)$$

$$\langle \rho_{R,R}(0) \rangle, \langle \rho_{L,L}(0) \rangle = \frac{1}{2}, \quad (28)$$

and the Hartree-Fock energy per particle is

$$E_{IC} = -\frac{1}{4} \left(\frac{e^2}{\kappa l_{\perp}} \right) [X(0) + \tilde{X}(0)], \quad (29)$$

which does not depend on the tunneling term or the parallel magnetic field.

C. Commensurate Stripe Phase (CSP)

In what follows, the parallel magnetic field is assumed to be in the \hat{y} direction so that $\mathbf{Q} = Q_0 \hat{\mathbf{x}}$. The coherent stripes are defined by charge and spin modulations with reciprocal lattice vectors $\mathbf{G} = \frac{2\pi}{a} n \hat{\mathbf{e}}$ where $n = 0, \pm 1, \pm 2, \dots$ and $\hat{\mathbf{e}}$ is a unit vector in a direction making an angle α with \mathbf{Q} and the x axis. In the absence of the parallel magnetic field, the coherent stripes would be described by the order parameters $\{\langle \rho_{i,j}(\mathbf{G}) \rangle\}$. With the field, the situation is slightly more complex since the tunneling term forces $\langle \rho_{R,L}(\mathbf{Q}) \rangle \neq 0$ and in general $\mathbf{Q} \notin \{\mathbf{G}\}$.

To apply our equation of motion method, we need a single set of wavevectors to describe the modulated state. This can be achieved by considering a solution for the transverse part of the spins, of the form

$$\langle \rho_{R,L}(\mathbf{r}) \rangle = e^{-i\mathbf{Q} \cdot \mathbf{r}} \langle \tilde{\rho}_{R,L}(\mathbf{r}) \rangle, \quad (30)$$

where $\langle \tilde{\rho}_{R,L}(\mathbf{r}) \rangle$ has the periodicity of the stripe state [i.e., $\langle \tilde{\rho}_{R,L}(\mathbf{r}) \rangle \neq 0$ for $\mathbf{q} \in \{\mathbf{G}\}$]. The sole effect of the rotating field is to force a rotation of the pseudospins in the xy plane in the stripe state which itself has the pseudospins rotating in the xz plane. We call this solution the commensurate stripe phase (CSP). Finding the order parameters is most easily accomplished by going into a spatially rotating frame where the xy pseudospins are aligned. We define the average values of the operators in the rotating frame by

$$\langle \tilde{\rho}_{R,L}(\mathbf{q}) \rangle \equiv \langle \rho_{R,L}(\mathbf{q} - \mathbf{Q}) \rangle, \quad (31)$$

$$\langle \tilde{\rho}_{L,R}(\mathbf{q}) \rangle \equiv \langle \rho_{L,R}(\mathbf{q} + \mathbf{Q}) \rangle. \quad (32)$$

Because the system of equations (9)-(12) contains the factor $\gamma_{\mathbf{q},\mathbf{q}'}$, making the substitution $\mathbf{q} \rightarrow \mathbf{q} \pm \mathbf{Q}$ introduces additional phase factors in the equations. We can preserve the structure of this system of equations in the rotating frame if we also redefine the diagonal order parameters as

$$\langle \tilde{\rho}_m^{R,R}(\mathbf{q}) \rangle \equiv \gamma^*(\mathbf{q}) \langle \rho_m^{R,R}(\mathbf{q}) \rangle, \quad (33)$$

$$\langle \tilde{\rho}_m^{L,L}(\mathbf{q}) \rangle \equiv \gamma(\mathbf{q}) \langle \rho_m^{L,L}(\mathbf{q}) \rangle, \quad (34)$$

where

$$\gamma(\mathbf{q}) \equiv e^{i\mathbf{q} \times \mathbf{Q} l_\perp^2/2} = e^{-iq_y Q l_\perp^2/2}. \quad (35)$$

The CSP thus occurs when $\langle \tilde{\rho}_m^{i,j}(\mathbf{q}) \rangle$ are non-vanishing for $\mathbf{q} \in \{\mathbf{G}\}$.

To carry out the computation, it is convenient to define a 2×2 Green's function matrix, with matrix elements

$$\tilde{G}_{R,L}(\mathbf{q}, \omega_n) \equiv G_{R,L}(\mathbf{q} + \mathbf{Q}, \omega_n), \quad (36)$$

$$\tilde{G}_{L,R}(\mathbf{q}, \omega_n) \equiv G_{L,R}(\mathbf{q} - \mathbf{Q}, \omega_n), \quad (37)$$

$$\tilde{G}_{R,R}(\mathbf{q}, \omega_n) \equiv \gamma^*(\mathbf{q}) G_{R,R}(\mathbf{q}, \omega_n), \quad (38)$$

$$\tilde{G}_{L,L}(\mathbf{q}, \omega_n) \equiv \gamma(\mathbf{q}) G_{L,L}(\mathbf{q}, \omega_n). \quad (39)$$

Using the fact that $\mathbf{Q} = Q \hat{\mathbf{x}}$, we have

$$t(\mathbf{q} \pm \mathbf{Q}) = t(\mathbf{q}). \quad (40)$$

With these definitions and identities, the system of equations for the single-particle Green's function in the rotating frame is

$$\begin{aligned} & \left[i\omega_n - \frac{1}{\hbar} (E_0 - \mu) \right] \tilde{G}_{R,R}(\mathbf{q}, \omega_n) + \frac{1}{\hbar} t(Q) \tilde{G}_{L,R}(\mathbf{q}, \omega_n) \\ & - \sum_{\mathbf{q}'} \tilde{U}_{R,R}(\mathbf{q}, \mathbf{q}') \tilde{G}_{R,R}(\mathbf{q}', \omega_n) - \sum_{\mathbf{q}'} \tilde{U}_{R,L}(\mathbf{q}, \mathbf{q}') \tilde{G}_{L,R}(\mathbf{q}', \omega_n) = \delta_{\mathbf{q},0}, \end{aligned} \quad (41)$$

$$\begin{aligned} & \left[i\omega_n - \frac{1}{\hbar} (E_0 - \mu) \right] \tilde{G}_{R,L}(\mathbf{q}, \omega_n) + \frac{1}{\hbar} t(Q) \tilde{G}_{L,L}(\mathbf{q}, \omega_n) \\ & - \sum_{\mathbf{q}'} \tilde{U}_{R,R}(\mathbf{q}, \mathbf{q}') \tilde{G}_{R,L}(\mathbf{q}', \omega_n) - \sum_{\mathbf{q}'} \tilde{U}_{R,L}(\mathbf{q}, \mathbf{q}') \tilde{G}_{L,L}(\mathbf{q}', \omega_n) = 0, \end{aligned} \quad (42)$$

$$\begin{aligned} & \left[i\omega_n - \frac{1}{\hbar} (E_0 - \mu) \right] \tilde{G}_{L,R}(\mathbf{q}, \omega_n) + \frac{1}{\hbar} t(Q) \tilde{G}_{R,R}(\mathbf{q}, \omega_n) \\ & - \sum_{\mathbf{q}'} \tilde{U}_{L,R}(\mathbf{q}, \mathbf{q}') \tilde{G}_{R,R}(\mathbf{q}', \omega_n) - \sum_{\mathbf{q}'} \tilde{U}_{L,L}(\mathbf{q}, \mathbf{q}') \tilde{G}_{L,R}(\mathbf{q}', \omega_n) = 0, \end{aligned} \quad (43)$$

$$\begin{aligned} & \left[i\omega_n - \frac{1}{\hbar} (E_0 - \mu) \right] \tilde{G}_{L,L}(\mathbf{q}, \omega_n) + \frac{1}{\hbar} t(Q) \tilde{G}_{R,L}(\mathbf{q}, \omega_n) \\ & - \sum_{\mathbf{q}'} \tilde{U}_{L,R}(\mathbf{q}, \mathbf{q}') \tilde{G}_{R,L}(\mathbf{q}', \omega_n) - \sum_{\mathbf{q}'} \tilde{U}_{L,L}(\mathbf{q}, \mathbf{q}') \tilde{G}_{L,L}(\mathbf{q}', \omega_n) = \delta_{\mathbf{q},0}. \end{aligned} \quad (44)$$

The four mean-field potentials, in this frame, are given by

$$\tilde{U}_{R,R}(\mathbf{q}, \mathbf{q}') = \gamma^*(\mathbf{q}) U_{R,R}(\mathbf{q}, \mathbf{q}') \gamma(\mathbf{q}'), \quad (45)$$

$$\tilde{U}_{L,L}(\mathbf{q}, \mathbf{q}') = \gamma(\mathbf{q}) U_{L,L}(\mathbf{q}, \mathbf{q}') \gamma^*(\mathbf{q}'), \quad (46)$$

$$\tilde{U}_{R,L}(\mathbf{q}, \mathbf{q}') = U_{R,L}(\mathbf{q} + \mathbf{Q}, \mathbf{q}') \gamma^*(\mathbf{q}'), \quad (47)$$

$$\tilde{U}_{L,R}(\mathbf{q}, \mathbf{q}') = U_{L,R}(\mathbf{q} - \mathbf{Q}, \mathbf{q}') \gamma(\mathbf{q}'). \quad (48)$$

Finally, the Hartree-Fock energy per particle is given by

$$\begin{aligned} E_{CSP} = & -\frac{2}{\nu} \sum_{\alpha} t_N(\mathbf{Q}) \operatorname{Re} [\langle \tilde{\rho}_{R,L}(0) \rangle] \\ & + \frac{1}{2\nu} \left(\frac{e^2}{\kappa l_{\perp}} \right) \sum_{\mathbf{q} \neq 0} H(\mathbf{q}) \left[|\langle \tilde{\rho}_{R,R}(\mathbf{q}) \rangle|^2 + |\langle \tilde{\rho}_{L,L}(\mathbf{q}) \rangle|^2 \right] \\ & - \frac{1}{2\nu} \left(\frac{e^2}{\kappa l_{\perp}} \right) \sum_{\mathbf{q}} X(\mathbf{q}) \left[|\langle \tilde{\rho}_{R,R}(\mathbf{q}) \rangle|^2 + |\langle \tilde{\rho}_{L,L}(\mathbf{q}) \rangle|^2 \right] \\ & + \frac{1}{\nu} \left(\frac{e^2}{\kappa l_{\perp}} \right) \sum_{\mathbf{q} \neq 0} \tilde{H}(\mathbf{q}) [\gamma^*(\mathbf{q})]^2 [\langle \tilde{\rho}_{R,R}(-\mathbf{q}) \rangle \langle \tilde{\rho}_{L,L}(\mathbf{q}) \rangle] \\ & - \frac{1}{\nu} \left(\frac{e^2}{\kappa l_{\perp}} \right) \sum_{\mathbf{q}} \tilde{X}(\mathbf{q} + \mathbf{Q}) |\langle \tilde{\rho}_{L,R}(\mathbf{q}) \rangle|^2. \end{aligned} \quad (49)$$

At fixed d/l_{\perp} and B_{\parallel} , the energy of the CSP is obtained by minimizing the Hartree-Fock energy of Eq. (49) with respect to a , the separation between the stripes in a given well (which may be written in unitless form as $\xi = a/l_{\perp}$) and with respect to the orientation α of the stripes with the x axis. When $\alpha \neq 0$, the commensurate rotation of the pseudospins will induce a modulation in the total density. As long as the rotation remains commensurate and has a single wavevector, however, the induced density will have the same periodicity as that of the stripes. This can be seen as follows. The relation between the topological charge and the pseudospin texture is given by

$$\delta \langle n(\mathbf{r}) \rangle = \frac{1}{8\pi} \varepsilon_{abc} S_a(\mathbf{r}) \varepsilon_{ij} \partial_i S_b(\mathbf{r}) \partial_j S_c(\mathbf{r}), \quad (50)$$

where ε_{ij} and ε_{abc} are antisymmetric tensors and $\mathbf{S}(\mathbf{r})$ is a classical field with unit modulus representing the pseudospins. If we write a general solution as

$$S_x(\mathbf{r}) = \sin[\theta(\mathbf{r})]\cos[\varphi(\mathbf{r})], \quad (51)$$

$$S_y(\mathbf{r}) = \sin[\theta(\mathbf{r})]\sin[\varphi(\mathbf{r})], \quad (52)$$

$$S_z(\mathbf{r}) = \cos[\theta(\mathbf{r})], \quad (53)$$

then the induced density takes the simple form

$$\delta n(\mathbf{r}) = \frac{1}{4\pi} \sin[\theta(\mathbf{r})] [\nabla\varphi(\mathbf{r}) \times \nabla\theta(\mathbf{r})] \cdot \hat{\mathbf{z}}. \quad (54)$$

Writing a general solution for $\varphi(\mathbf{r})$ in the form

$$\varphi(\mathbf{r}) = \tilde{\varphi}(\mathbf{r}) + \mathbf{Q} \cdot \mathbf{r}, \quad (55)$$

the induced density can be written as

$$\delta n(\mathbf{r}) = \frac{1}{4\pi} \sin[\theta(\mathbf{r})] [\nabla\tilde{\varphi}(\mathbf{r}) \times \nabla\theta(\mathbf{r}) + \mathbf{Q} \times \nabla\theta(\mathbf{r})] \cdot \hat{\mathbf{z}}. \quad (56)$$

In the CSP and ISP, $\tilde{\varphi}(\mathbf{r}) = 0$ and so

$$\delta n(\mathbf{r}) = \frac{1}{4\pi} \sin[\theta(\mathbf{r})] [\mathbf{Q} \times \nabla\theta(\mathbf{r})] \cdot \hat{\mathbf{z}}. \quad (57)$$

There is no induced charge for stripes aligned with the parallel field [i.e. $\mathbf{Q} \parallel \nabla\theta(\mathbf{r})$]. For other orientations of the stripes, the induce charge has the same periodicity as that of the angle $\theta(\mathbf{r})$ that defines the staggered magnetization in the xz plane.

In our Hartree-Fock calculation, we find that the most favorable configuration is that of the stripes aligned with the parallel magnetic field. The same conclusion was also reported previously by Demler et al.¹⁴. Thus, we will choose $\alpha = 0$ in the rest of this paper.

D. Incommensurate Stripe Phase (ISP)

In analogy with the IL state, we define an incommensurate stripe phase (ISP) by the absence of rotation of the spins in the xy plane. This state is most naturally described by the original order parameters $\langle \rho_{ij}(\mathbf{q}) \rangle$ which, together with $G_{L,R}(\mathbf{q}, \omega_n)$, are non-vanishing for $\mathbf{q} \in \{\mathbf{G}\}$. In particular, $G_{L,R}(\mathbf{q} - \mathbf{Q}, \omega_n) = 0$ for any $\mathbf{q} \in \{\mathbf{G}\}$ so that the tunneling term in Eqs. (9)-(12) is zero. The order parameters of the ISP are thus found by solving directly Eqs. (9)-(12) with $t(\mathbf{q}) = 0$ (or, alternatively, Eqs. (41)-(44) with $t_N(Q) = 0$ and $\mathbf{Q} = 0$). While this is not an exact solution to the Hartree-Fock equations, what is ignored are the remnants of the solitons of the SLS which are relatively dense and leave only a very weak modulation of the pseudospin, except quite close to the transition out of the CSP state¹³. Setting $t(\mathbf{q}) = 0$ effectively ignores this weak modulation, and introduces a great simplification in the numerics. The resulting energy one finds for the ISP does not depend on the parallel magnetic field, just as for the IL state. We note that, because of the absence of tunneling in the Hartree-Fock equations, our approximate form of the ISP is equivalent to the coherent stripe state studied in Refs. 6 and 9.

V. PHASE DIAGRAM IN LANDAU LEVEL $N = 2$

In the Hartree-Fock approximation, the transition between the CL to the IL states occurs when $E_{CL} = E_{IL}$ or, equivalently, when

$$\frac{\frac{1}{4} \left[\tilde{X}(0) - \tilde{X}(\mathbf{Q}) \right] e^{Q^2 \ell_{\perp}^2 / 4}}{\left| L_n^0 \left(\frac{Q^2 \ell_{\perp}^2}{2} \right) \right|} = \frac{t_0}{(e^2 / \kappa \ell)}. \quad (58)$$

In Fig. 1, we show the contour lines in the $d - B_{\parallel}$ plane separating the CL from the IL for several values of the tunneling parameter. (We assume a typical density of $n = 1 \times 10^{11} \text{ cm}^{-2}$ in our calculation and in all the graphs presented

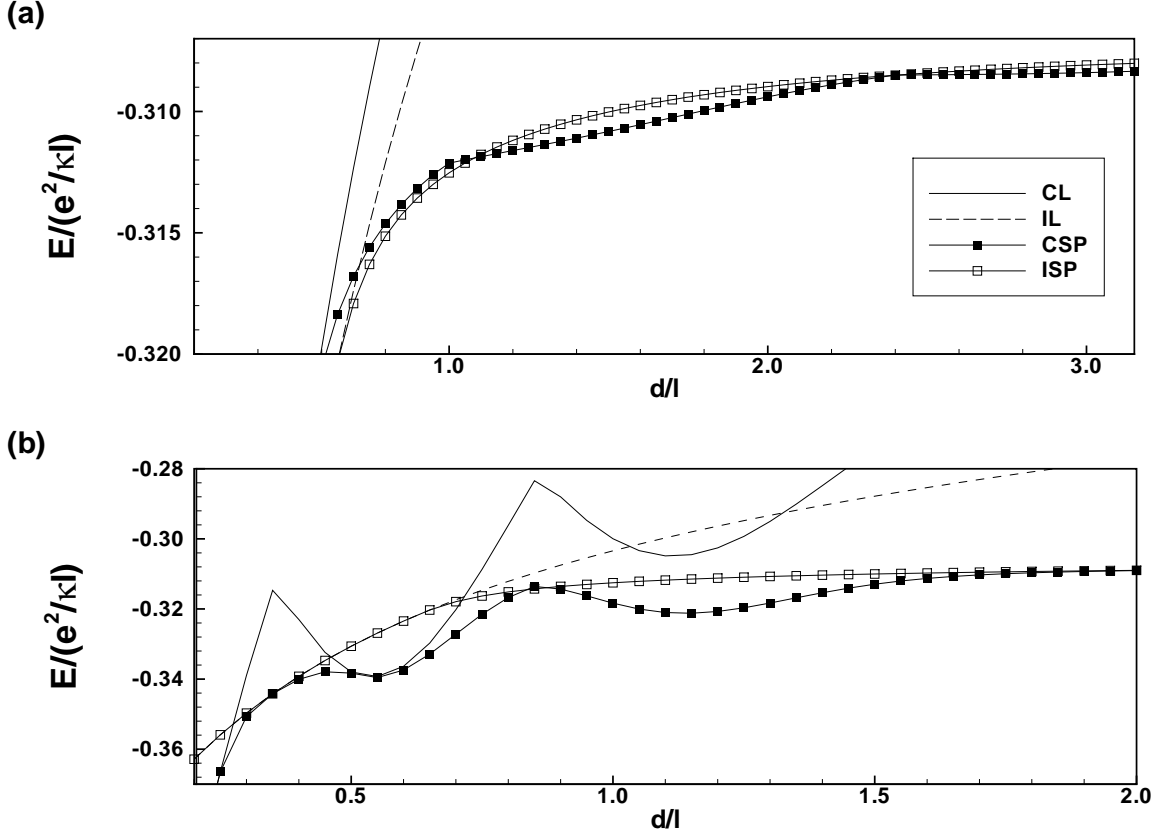


FIG. 5: Energy per electron in the liquid and stripe phases as a function of the separation between the wells for $N = 2$ and (a) $t_0/(e^2/\kappa\ell) = 0.01$, $B_{\parallel} = 0.5$ T and (b) $t_0/(e^2/\kappa\ell) = 0.1$, $B_{\parallel} = 1.4$ T.

in this paper). We remark that the oscillations of $t_N(Q)$ lead to a complex sequence of transitions between the two liquid states with two reentrant CL phases for $N = 2$. We do not analyse these transitions in further detail, however, because at a value of $d > d_c(B_{\parallel})$, the liquid states are higher in energy than the stripe states as indicated in Fig. 1, and the value of $d_c(B_{\parallel})$ is lower than the value of d at which the reentrant CL states appear. It is nevertheless an interesting possibility that these reentrant transitions might occur when Landau level mixing or finite well thickness effects are included in the calculation.

When stripe phases are taken into account, the phase diagram becomes even more complex because the oscillations of $t_N(Q)$ also produce reentrant CSP and ISP states. Figure 5 shows the variation of the energy of the four states with respect to d for some typical cases. The interchange of the ISP and CSP is clearly visible in Fig. 5(a). The line called $d_c(B_{\parallel})$ in Fig. 1 indicates the transition from one of the liquid states to one of the stripe states (either CSP or ISP). At small value of t_0 , d_c is almost independent of B_{\parallel} . At larger values of d or B_{\parallel} where $t_N(Q) \rightarrow 0$, the amplitude of the pseudo-magnetic field goes to zero and there is no gain in tunneling energy for the pseudospins to rotate. On the contrary, there is only an exchange energy cost. It is thus clear that the ground state must be the ISP at large d or B_{\parallel} and the CSP only exists in a limited parameter region. Note however that, at large value of d , the LCR's are very narrow and the cost of the commensurate rotation in exchange energy is very small. The difference between the CSP and ISP energies in this limit is close to our numerical accuracy as can be seen in for large d in Fig. 5(b) and large B_{\parallel} in Fig. 6(a).

From an experimental point of view, it is more interesting to study the behavior of the energy of the four states with respect to B_{\parallel} at a fixed value of d . Referring to Fig. 1(a), we choose, for $t_0 = 0.01$, $d/\ell_{\perp} = 1.4$, a value greater than $d_c(B_{\parallel})$ so that the ground state is one of the stripe states. We plot, in Fig. 6: (a) the energy of the CSP and ISP, (b) the variation in $t_N(Q)$, and (c) the corresponding variation of the order parameters $\langle \tilde{\rho}_{R,L}(0) \rangle_{CSP}$ and $\langle \rho_{R,L}(0) \rangle_{ISP}$. (We remark that, in the CL, $\langle \tilde{\rho}_{R,L}(0) \rangle = 0.5$ and $\langle \rho_{R,L}(0) \rangle = 0$ while in the IL, $\langle \tilde{\rho}_{R,L}(0) \rangle = 0$ and $\langle \rho_{R,L}(0) \rangle = 0.5$). In the specific case studied in Fig. 6, the ground state goes through the sequence CSP-ISP-CSP-ISP-CSP-ISP when B_{\parallel} is increased. A change in the sign of $t_N(Q)$ leads to a cusp in the curve of the energy of the

CSP and to a corresponding change in sign in $\langle \tilde{\rho}_{R,L}(0) \rangle$. With our choice of phase, the pseudospins are oriented along x in the rotating frame for the CSP. When $t_N(Q)$ changes sign, the corresponding effective magnetic field is reversed and the pseudospins then point along $-x$. In computing Fig. 6, we have included only the CSP and ISP. But, we know from the study of the effect of B_{\parallel} on the ground state at $\nu = 1$ that the commensurate state does not go directly into the incommensurate state. At a certain $B_{\parallel} = B_{\parallel,CL-SLS}$, which is smaller than the value $B_{\parallel} = B_{\parallel,CL-IL}$ at which the $CL-IL$ transition occurs, the commensurate state becomes unstable towards the formation of solitons. For $B_{\parallel} > B_{\parallel,CL-SLS}$, the ground state contains a finite density of these defects. They form a soliton lattice whose lattice spacing depends on B_{\parallel} . In analogy with the case $\nu = 1$, we expect that the same scenario will repeat itself here whenever the CSP approaches the ISP from below or above. A precursor of this instability is seen in the softening of the low-energy modes of the CSP as described below¹⁵.

There are many possible transitions between the four states kept in our analysis. In Fig. 1, we indicate all transitions between the CL and IL states, but not all transitions into commensurate or incommensurate stripe phases that occur for $d > d_c$. In general, we expect transitions between the CSP and the ISP whenever the tunneling matrix element becomes small, as occurs in the liquid states. Thus, just as we see d_c occurs near the first CL-IL transition in Fig. 1, we expect higher order CSP-ISP transitions near what are shown as the reentrant CL-IL transitions. Clearly, this system supports a remarkably rich phase diagram.

How might one detect these phase transitions in experiment? One possibility, as we discuss below, is to study the behavior of the tunneling current with the parallel magnetic field. As we shall see this affords a clear signature of the transition between liquid and stripe phases. To compute the tunneling current, we need to know the collective excitations and response functions related to the density and pseudospin orders. We address this question in the next section.

VI. RESPONSE FUNCTIONS IN THE TIME-DEPENDENT HARTREE-FOCK APPROXIMATION

As mentioned above, the collective modes are important in determining the tunneling current in the double layer system in response to an interlayer bias potential. Their dispersions can also be measured experimentally via inelastic light scattering. To derive them, we compute the retarded density and pseudospin response functions, and track their poles. The response functions are obtained by analytical continuation of the two-particle Matsubara Green's functions

$$\chi_{i,j,k,l}(\mathbf{q}, \mathbf{q}'; \tau) = -N_{\phi} \langle T \rho_{i,j}(\mathbf{q}, \tau) \rho_{k,l}(-\mathbf{q}', 0) \rangle + N_{\phi} \langle \rho_{i,j}(\mathbf{q}) \rangle \langle \rho_{k,l}(-\mathbf{q}') \rangle. \quad (59)$$

The response functions $\chi_{i,j,k,l}(\mathbf{q}, \mathbf{q}'; \tau)$ are computed in the time-dependent Hartree-Fock approximation. The calculation we do here is a generalization of that presented in Refs. 9 and 13. To include the parallel field and so the commensurate rotation, it is necessary to derive the equation of motion for the matrix of response functions defined in the rotating frame by

$$\tilde{P}(\mathbf{q}, \mathbf{q}'; i\Omega_n) \equiv \begin{pmatrix} \gamma^* \chi_{R,R,R,R}(\mathbf{q}, \mathbf{q}') \gamma & \gamma^* \chi_{R,R,L,R}(\mathbf{q}, \mathbf{q}' - \mathbf{Q}) & \gamma^* \chi_{R,R,R,L}(\mathbf{q}, \mathbf{q}' + \mathbf{Q}) & \gamma^* \chi_{R,R,L,L}(\mathbf{q}, \mathbf{q}') \gamma^* \\ \chi_{R,L,R,R}(\mathbf{q} - \mathbf{Q}, \mathbf{q}') \gamma & \chi_{R,L,L,R}(\mathbf{q} - \mathbf{Q}, \mathbf{q}' - \mathbf{Q}) & \chi_{R,L,R,L}(\mathbf{q} - \mathbf{Q}, \mathbf{q}' + \mathbf{Q}) & \chi_{R,L,L,L}(\mathbf{q} - \mathbf{Q}, \mathbf{q}') \gamma^* \\ \chi_{L,R,R,R}(\mathbf{q} + \mathbf{Q}, \mathbf{q}') \gamma & \chi_{L,R,L,R}(\mathbf{q} + \mathbf{Q}, \mathbf{q}' - \mathbf{Q}) & \chi_{L,R,R,L}(\mathbf{q} + \mathbf{Q}, \mathbf{q}' + \mathbf{Q}) & \chi_{L,R,L,L}(\mathbf{q} + \mathbf{Q}, \mathbf{q}') \gamma^* \\ \gamma \chi_{L,L,R,R}(\mathbf{q}, \mathbf{q}') \gamma & \gamma \chi_{L,L,L,R}(\mathbf{q}, \mathbf{q}' - \mathbf{Q}) & \gamma \chi_{L,L,R,L}(\mathbf{q}, \mathbf{q}' + \mathbf{Q}) & \gamma \chi_{L,L,L,L}(\mathbf{q}, \mathbf{q}') \gamma^* \end{pmatrix} \quad (60)$$

where γ on the left(right) of $\tilde{P}(\mathbf{q}, \mathbf{q}'; \Omega_n)$ stands for $\gamma(\mathbf{q})(\gamma(\mathbf{q}'))$ and Ω_n is a Matsubara bosonic frequency. In the time-dependent Hartree-Fock approximation (TDHFA), the summation of ladders and bubble diagrams gives

$$\tilde{P}(\mathbf{q}, \mathbf{q}'; i\Omega_n) = \tilde{P}^0(\mathbf{q}, \mathbf{q}'; i\Omega_n) + \frac{1}{\hbar} \sum_{\mathbf{q}''} \tilde{P}^0(\mathbf{q}, \mathbf{q}''; i\Omega_n) Y(\mathbf{q}'') \tilde{P}(\mathbf{q}'', \mathbf{q}'; i\Omega_n). \quad (61)$$

The vertex corrections involve the matrix of interactions

$$Y(\mathbf{q}) = \left(\frac{e^2}{\kappa l_{\perp}} \right) \begin{pmatrix} H(\mathbf{q}) - X(\mathbf{q}) & 0 & 0 & \tilde{H}(\mathbf{q}) [\gamma^*(\mathbf{q})]^2 \\ 0 & -\tilde{X}_-(\mathbf{q}) & 0 & 0 \\ 0 & 0 & -\tilde{X}_+(\mathbf{q}) & 0 \\ \tilde{H}(\mathbf{q}) [\gamma(\mathbf{q})]^2 & 0 & 0 & H(\mathbf{q}) - X(\mathbf{q}) \end{pmatrix}, \quad (62)$$

where we have defined

$$\tilde{X}_{\pm}(\mathbf{q}) = \tilde{X}(\mathbf{q} \pm \mathbf{Q}). \quad (63)$$

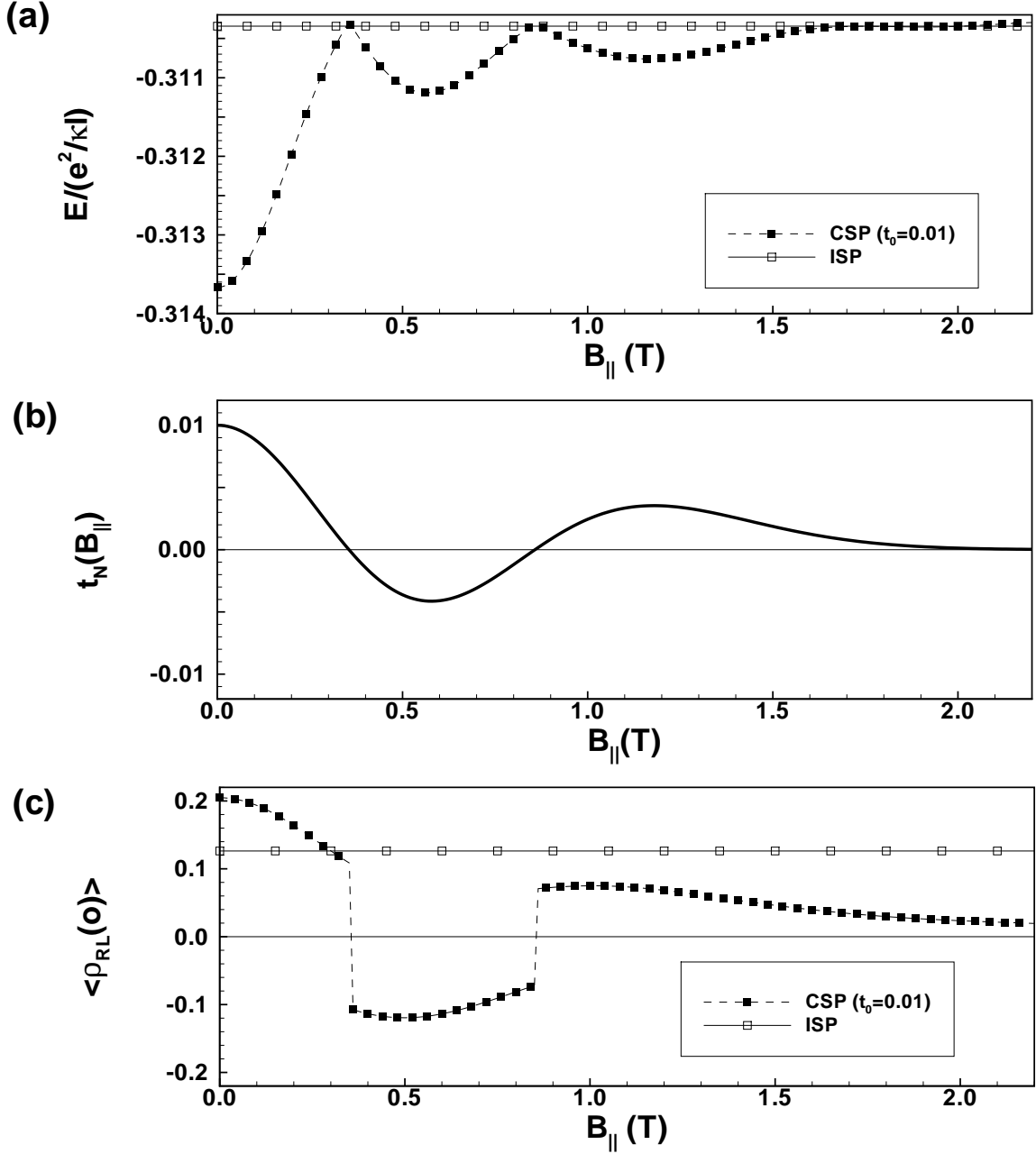


FIG. 6: Study of the CSP-ISP transition at $N = 2$ for $t_0 = 0.01$ and $d/\ell_\perp = 1.4$ showing (a) the variation of the energy of these two phases with B_{\parallel} , (b) the variation of the tunneling amplitude $t_N(Q)$ with B_{\parallel} and (c) the variations of the order parameters $\langle \tilde{\rho}_{R,L}(0) \rangle_{CSP}$ and $\langle \rho_{R,L}(0) \rangle_{ISP}$ with B_{\parallel} .

Using the Hartree-Fock Hamiltonian, H_{HF} , written in terms of the $\langle \rho_{i,j}(\mathbf{q}) \rangle$, we obtain an equation of motion for the Hartree-Fock response functions $\tilde{P}^0(\mathbf{q}, \mathbf{q}'; i\Omega_n)$ using $\frac{\partial}{\partial \tau}(\dots) = [H_{HF} - \mu N, (\dots)]$. Combining with Eq. (61), we obtain after a lengthy calculation an equation of motion for the TDHFA response functions than can be put in the simple matrix form

$$\sum_k \sum_{\mathbf{q}''} [i\hbar\Omega_n \delta_{i,k} \delta_{\mathbf{q}, \mathbf{q}''} - F_{i,k}(\mathbf{q}, \mathbf{q}'')] \tilde{P}_{k,j}(\mathbf{q}'', \mathbf{q}') = D_{i,j}(\mathbf{q}, \mathbf{q}'). \quad (64)$$

For completeness, we give the definitions of the matrices F and D in the Appendix. Notice that the dynamical response can be computed from a knowledge of the static order parameters $\{\langle \rho_{i,j}(\mathbf{q}) \rangle\}$ alone.

A. Response Functions of the Commensurate Liquid

For the CL, we can solve analytically Eq. (64) to get (after the analytical continuation $i\Omega_n \rightarrow \omega + i\delta$ and with $\zeta = \text{sign}[t_N(Q)]$)

$$\begin{aligned} & \begin{pmatrix} \chi_{R,R,R,R}(\mathbf{q}, \mathbf{q}') & \chi_{R,R,L,R}(\mathbf{q}, \mathbf{q}' - \mathbf{Q}) & \chi_{R,R,R,L}(\mathbf{q}, \mathbf{q}' + \mathbf{Q}) & \chi_{R,R,L,L}(\mathbf{q}, \mathbf{q}') \\ \chi_{R,L,R,R}(\mathbf{q} - \mathbf{Q}, \mathbf{q}') & \chi_{R,L,L,R}(\mathbf{q} - \mathbf{Q}, \mathbf{q}' - \mathbf{Q}) & \chi_{R,L,R,L}(\mathbf{q} - \mathbf{Q}, \mathbf{q}' + \mathbf{Q}) & \chi_{R,L,L,L}(\mathbf{q} - \mathbf{Q}, \mathbf{q}') \\ \chi_{L,R,R,R}(\mathbf{q} + \mathbf{Q}, \mathbf{q}') & \chi_{L,R,L,R}(\mathbf{q} + \mathbf{Q}, \mathbf{q}' - \mathbf{Q}) & \chi_{L,R,R,L}(\mathbf{q} + \mathbf{Q}, \mathbf{q}' + \mathbf{Q}) & \chi_{L,R,L,L}(\mathbf{q} + \mathbf{Q}, \mathbf{q}') \\ \chi_{L,L,R,R}(\mathbf{q}, \mathbf{q}') & \chi_{L,L,L,R}(\mathbf{q}, \mathbf{q}' - \mathbf{Q}) & \chi_{L,L,R,L}(\mathbf{q}, \mathbf{q}' + \mathbf{Q}) & \chi_{L,L,L,L}(\mathbf{q}, \mathbf{q}') \end{pmatrix} \quad (65) \\ & = \frac{(\zeta/2)\delta_{\mathbf{q},\mathbf{q}'}}{\hbar[(\omega + i\delta)^2 - \omega_{CL}^2(\mathbf{q})]} \begin{pmatrix} (b+c) & -\hbar(\omega + i\delta)\gamma & \hbar(\omega + i\delta)\gamma & -(b+c)\gamma^2 \\ -\hbar(\omega + i\delta)\gamma^* & 2\text{Re}(a) & -2\text{Re}(a) & \hbar(\omega + i\delta)\gamma \\ \hbar(\omega + i\delta)\gamma^* & -2\text{Re}(a) & 2\text{Re}(a) & -\hbar(\omega + i\delta)\gamma \\ -(\gamma^*)^2(b+c) & \hbar(\omega + i\delta)\gamma^* & -\hbar(\omega + i\delta)\gamma^* & +(b+c) \end{pmatrix}, \end{aligned}$$

where

$$a(\mathbf{q}) = \frac{1}{2}\zeta \left[2|t_N(Q)| + \left(\frac{e^2}{\kappa l_\perp} \right) \tilde{X}(Q) + \left(\frac{e^2}{\kappa l_\perp} \right) (H(q) - X(q) - \tilde{H}(q)e^{-i\mathbf{q}\times\mathbf{Q}l_\perp^2}) \right], \quad (66)$$

$$b(\mathbf{q}) = \frac{1}{2}\zeta \left[2|t_N(Q)| + \left(\frac{e^2}{\kappa l_\perp} \right) [\tilde{X}(Q) - \tilde{X}_+(q)] \right], \quad (67)$$

$$c(\mathbf{q}) = \frac{1}{2}\zeta \left[2|t_N(Q)| + \left(\frac{e^2}{\kappa l_\perp} \right) [\tilde{X}(Q) - \tilde{X}_-(q)] \right]. \quad (68)$$

There is a unique collective mode corresponding to an elliptical motion of the pseudospins about the x axis, in the yz plane, with a frequency given by

$$\hbar\omega_{CL}(\mathbf{q}) = \sqrt{[a(\mathbf{q}) + a^*(\mathbf{q})][b(\mathbf{q}) + c(\mathbf{q})]} \quad (69)$$

(We remark that, for $\mathbf{q} = 0$, $H(\mathbf{q}) - \tilde{H}(\mathbf{q}) \cos[\mathbf{q} \times \mathbf{Q}l_\perp^2] \rightarrow -d/\ell_\perp$). Note $\omega_{CL}(\mathbf{q})$ tends to a finite value for any $t_N(\mathbf{Q}) > 0$ in the long-wavelength limit¹⁶.

B. Response Functions of the Incommensurate Liquid

For the IL, the response functions are obtained by setting $t_N(Q) = 0$ and $Q = 0$. We get

$$\begin{aligned} & \begin{pmatrix} \chi_{R,R,R,R}(\mathbf{q}, \mathbf{q}') & \chi_{R,R,L,R}(\mathbf{q}, \mathbf{q}') & \chi_{R,R,R,L}(\mathbf{q}, \mathbf{q}') & \chi_{R,R,L,L}(\mathbf{q}, \mathbf{q}') \\ \chi_{R,L,R,R}(\mathbf{q}, \mathbf{q}') & \chi_{R,L,L,R}(\mathbf{q}, \mathbf{q}') & \chi_{R,L,R,L}(\mathbf{q}, \mathbf{q}') & \chi_{R,L,L,L}(\mathbf{q}, \mathbf{q}') \\ \chi_{L,R,R,R}(\mathbf{q}, \mathbf{q}') & \chi_{L,R,L,R}(\mathbf{q}, \mathbf{q}') & \chi_{L,R,R,L}(\mathbf{q}, \mathbf{q}') & \chi_{L,R,L,L}(\mathbf{q}, \mathbf{q}') \\ \chi_{L,L,R,R}(\mathbf{q}, \mathbf{q}') & \chi_{L,L,L,R}(\mathbf{q}, \mathbf{q}') & \chi_{L,L,R,L}(\mathbf{q}, \mathbf{q}') & \chi_{L,L,L,L}(\mathbf{q}, \mathbf{q}') \end{pmatrix} \quad (70) \\ & = \frac{(1/2)\delta_{\mathbf{q},\mathbf{q}'}}{\hbar[(\omega + i\delta)^2 - \omega_{IL}^2(\mathbf{q})]} \begin{pmatrix} 2B & -\hbar(\omega + i\delta) & \hbar(\omega + i\delta) & -2B \\ -\hbar(\omega + i\delta) & 2A & -2A & \hbar(\omega + i\delta) \\ \hbar(\omega + i\delta) & -2A & 2A & -\hbar(\omega + i\delta) \\ -2B & \hbar(\omega + i\delta) & -\hbar(\omega + i\delta) & 2B \end{pmatrix}, \end{aligned}$$

where

$$A(\mathbf{q}) = \frac{1}{2} \left(\frac{e^2}{\kappa l_\perp} \right) [H(\mathbf{q}) - \tilde{H}(\mathbf{q}) + \tilde{X}(0) - X(\mathbf{q})], \quad (71)$$

$$B(\mathbf{q}) = \frac{1}{2} \left(\frac{e^2}{\kappa l_\perp} \right) [\tilde{X}(0) - \tilde{X}(\mathbf{q})]. \quad (72)$$

The collective mode is gapless and given by

$$\hbar\omega_{IL}(\mathbf{q}) = 2\sqrt{A(\mathbf{q})B(\mathbf{q})}. \quad (73)$$

To linear order in q (and for $d \neq 0$), this becomes

$$\hbar\omega_{IL}(\mathbf{q}) \approx q \left(\frac{e^2}{\kappa l_\perp} \right) \sqrt{\left(\frac{-1}{2} \right) \frac{\partial^2 \tilde{X}(k)}{\partial k^2} \Big|_{k=0}} \left(\tilde{X}(0) - X(0) + \frac{d}{\ell_\perp} \right) \quad (74)$$

Thus for long wavelengths the dispersion is linear in q and gapless even if $t > 0$.

C. Response Functions in the Commensurate Stripe Phase

We study the dispersion relation of the lower-energy collective modes of the CSP by a numerical solution of the system of equations given by Eq. (64). In the absence of tunneling and parallel magnetic field, there are two Goldstone modes⁹. One is a phonon mode with an in-phase motion of the density of the stripes in the two wells accompanied by an $x - z$ motion of the pseudospins. The second is a pseudospin wave mode with an out-of-phase motion of the densities and a small rotation of the pseudospins about their equilibrium position. As explained in Ref. 9, the low-energy modes can be described by a pseudospin-wave theory where the effective periodicity is set by the separation between neighboring linear coherent regions (LCR's) which is half the separation between the stripes in a given layer. If we take the the Brillouin zone edges (in the x direction) to be $\pm 2\pi/a$ instead of $\pm\pi/a$, then the phonon and pseudospin wave mode are both part of the same low-energy mode, the former dispersing from the zone center and the latter from the zone edge. This is very clearly seen from Fig. 2(a) and Fig. 2(b) where we show the full dispersion relation of these modes in the ISP and in the CSP with $B_{\parallel} = 0$ T. In Fig. 2(b), we see that the gap at the zone edge (and so in the pseudospin wave mode) is strongly increased from its bare value $2t_0$ by self-energy and vertex corrections. The phonon, by contrast, has vanishing energy at the zone center. For $B_{\parallel} = 0$, the phonon mode has $\omega(k_{\parallel}, k_{\perp} = 0) \sim k_{\parallel}^2$ and $\omega(k_{\parallel} = 0, k_{\perp}) \sim k_{\perp}$ and is independent of t_0 . For $B_{\parallel} = 0$ and $t_0 = 0$, the pseudospin wave mode has $\omega(k_{\parallel}, k_{\perp} = 0) \sim k_{\parallel}$, $\omega(k_{\parallel} = 0, k_{\perp}) \sim k_{\perp}$ (see Ref. 9).

In Fig. 6, we showed the behavior of the renormalized tunneling term, $t_N(Q)$, as B_{\parallel} is increased at $d/\ell_{\perp} = 1.4$ for $N = 2$. We now look at the corresponding behavior of the dispersion relation for the phonon and pseudospin wave modes. (As discussed above, these two modes are both part of the same collective mode in an extended Brillouin zone such as that used in Fig. 7). Figure 7 shows the dispersion relations of these collective excitations as B_{\parallel} is increased until slightly above the first value where $t_N(Q) = 0$ where the system is in the ISP. The parallel field has an important effect on the lowest-energy modes. The gap in the pseudospin mode (the part of the dispersion near the zone edge in Fig. 7) is progressively closed as $t_N(Q) \rightarrow 0$. But, these modes do not become completely dispersionless along $k_{\parallel} = 0$. Before the CSP-ISP transition, these low-energy modes become unstable at the zone center at some value $B_{\parallel}^* < B_{\parallel,CSP-ISP}$. The instability persists in a small region around $B_{\parallel,CSP-ISP}$. (For the case represented in Fig. 6, we found that the first instability region is from $B_{\parallel} = 0.34$ to $B_{\parallel} = 0.40$). Above $B_{\parallel,CSP-ISP}$, the ground state is stable again and the gap increases and decreases again until the next zero of $t_N(Q) = 0$ where the same scenario is repeated. Finally, just before the final transition from the CSP to the ISP, i.e. at $B_{\parallel} = 1.6$ for the case represented in Fig. 6, the CSP becomes unstable again.

In analogy with the case of filling factor $\nu = 1$, we expect that these instabilities are precursors of a transition from the CSP to a soliton lattice state. For $\nu = 1$, the instability occurs for $B_{\parallel}^* > B_{\parallel,CL-SLS}$ and the transition from the commensurate liquid to the SLS is first order. We do not know if this is the case for the CSP to ISP transition as we could not calculate $B_{\parallel,CSP-SLS}$ with our Hartree-Fock method. In any case, these instabilities need not be worried about when considering the low energy spectrum: the introduction of solitons into the groundstate will open gaps in the collective mode spectrum at various values of k_{\perp} , but should not provide any new gapless modes since translational symmetry has already been broken by the stripes.

Figure 8 shows the dispersion relation of the collective modes in the direction of the stripes for several values of the parallel magnetic field. It is clear that a change in B_{\parallel} has a profound impact on the long-wavelength dispersion of the phase mode (lowest energy gapped mode at $k_{\parallel} = 0$) as well as on the roton minimum. In contrast, the higher-energy modes are much less affected by the parallel field. (This is also true for dispersion perpendicular to the stripes). The phase mode becomes nearly linear in k_{\parallel} at $k_{\perp} = 0$ near the zeros of $t_N(Q)$. The long-wavelength phonon dispersion changes slowly with B_{\parallel} . At small B_{\parallel} , we find $\omega(k_{\parallel} \rightarrow 0, k_{\perp} = 0) \sim k_{\parallel}^2$ while at $B_{\parallel} = 0.8$ T (and for $d/\ell_{\perp} = 1.4$), the dispersion crosses over from quadratic to linear in k_{\parallel} at a relatively small value of k_{\parallel} [see Fig. 8(d)].

As the separation between the wells increases, both the CSP and ISP are unstable and the true ground state is that of a modulated stripe state described in Ref. 9. For $t_0/(e^2/\kappa\ell) = 0.01$, we find that the critical spacing is $d/\ell_{\perp} \approx 2.0$.

VII. TUNNELING RESPONSE IN THE COMMENSURATE STRIPE STATE

In this section we compute the interlayer tunneling $I - V$ to second order in the tunneling matrix element t_0 . Since t_0 is assumed to be small, the commensurate states can only exist in a very narrow range of parameters d and B_{\parallel} , so that they may effectively be ignored. We are thus interested in the IL-ISP transition, and whether there are distinguishable signatures of these two phases in the tunneling $I - V$. Recent work^{2,10} has demonstrated that a peak in the tunneling $I - V$ as a function of B_{\parallel} maps out the Goldstone mode associated with spontaneous interlayer coherence in the IL. As we now show, this result generalizes to the ISP, and the behavior of the peak with B_{\parallel} clearly

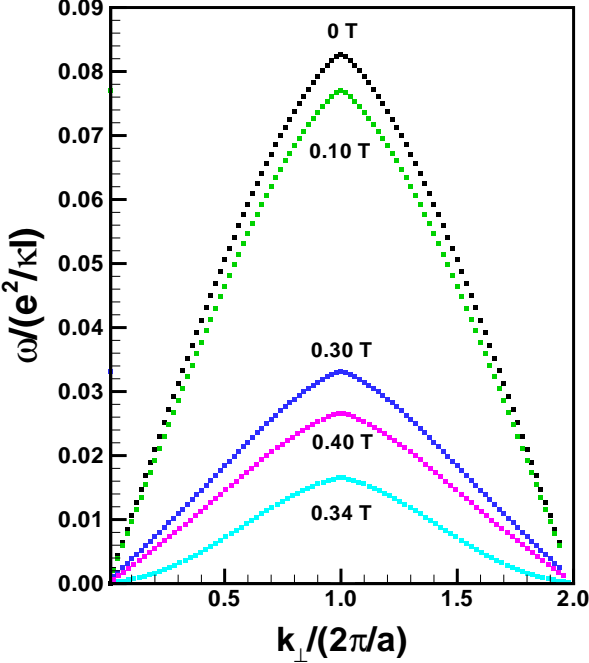


FIG. 7: Dispersion relation $\omega (k_{\parallel} = 0, k_{\perp})$ of the lowest-energy collective mode in the CSP for $N = 2, t_0 / (e^2 / \kappa \ell) = 0.01, d / \ell_{\perp} = 1.4$ and several values of the parallel magnetic field. The $[2\pi/a, 4\pi/a]$ region can be translated left by $2\pi/a$ to give the pseudospin wave dispersion.

distinguishes the two phases.

Our formalism closely follows that of Mahan¹⁷. The tunneling current is defined by

$$I(t) = -e \frac{dN_L}{dt} = +e \frac{dN_R}{dt}, \quad (75)$$

where $N_{L(R)} = \sum_X c_{X,L(R)}^\dagger c_{X,L(R)} = N_\phi \rho_{L(R),L(R)}(\mathbf{q} = 0)$ is the number of electrons in the left (right) well. $I(t)$ represents the interlayer current in the presence of a bias voltage while the tunneling operator connecting the two layers is adiabatically switched on, reaching its full value at time $t = 0$. The complete Hamiltonian of the system, including a bias between the wells, is written as

$$H = H' + H_T = H_0 - \mu_L N_L - \mu_R N_R + H_T, \quad (76)$$

where $eV = \mu_L - \mu_R$ is the potential bias and H_T is the tunneling hamiltonian given in Eq. (??). Written in terms of the ρ operators, it takes the form ($\mathbf{Q} = Q\hat{x}$)

$$H_T = -N_\phi t_N(Q) [\rho_{R,L}(-\mathbf{Q}) + \rho_{L,R}(\mathbf{Q})]. \quad (77)$$

The term H_0 in H contains the Coulomb interaction and kinetic energies. Since H_T is the only term that can change particle numbers in one well, we have

$$\frac{dN_R}{dt} = i [H_T, N_R] = \frac{i}{\hbar} N_\phi t_N(Q) [\rho_{R,L}(-\mathbf{Q}) - \rho_{L,R}(\mathbf{Q})]. \quad (78)$$

In all four states considered in this paper, $\langle \rho_{R,L}(-\mathbf{Q}) \rangle = \langle \rho_{L,R}(\mathbf{Q}) \rangle$ so that there is no current in the ground state. Using standard linear response theory¹⁷, the current is given by

$$\langle I(t) \rangle = \frac{i}{\hbar} \int_{-\infty}^t dt' \left\langle \left[\tilde{H}_T(t'), \tilde{I}(t) \right] \right\rangle_{H'}, \quad (79)$$

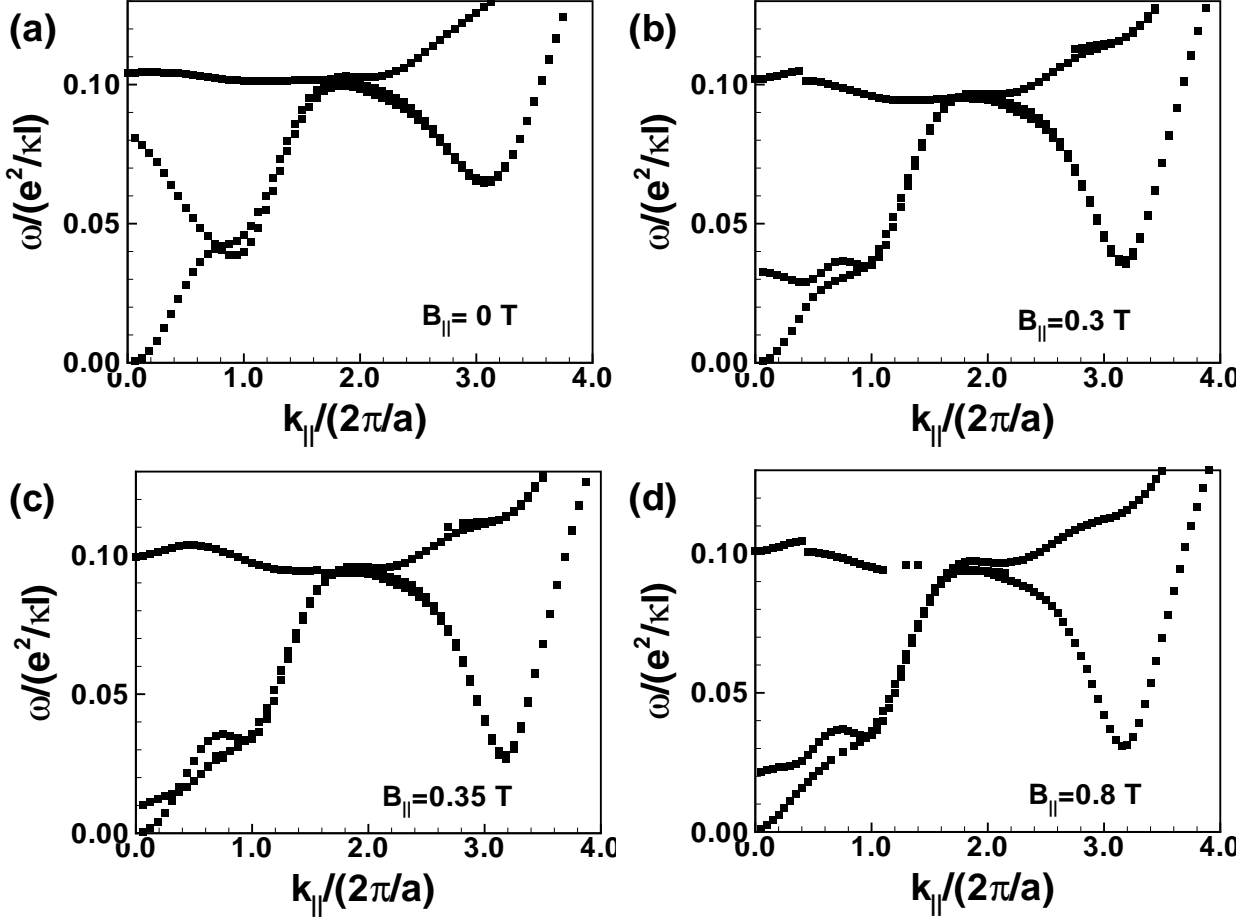


FIG. 8: Evolution of the dispersion relations $\omega(k_{\parallel}, k_{\perp} = 0)$ of the lowest-energy collective modes of the CSP as a function of the parallel magnetic field for $N = 2$, $t_0/(e^2/\kappa l) = 0.01$ and $d/\ell_{\perp} = 1.4$.

where the time dependence of the operators is given by $\tilde{I}(t) = e^{iH't/\hbar} I(0) e^{-iH't/\hbar}$. After some algebra, we find the familiar result

$$I(t) = -2 \frac{e}{\hbar^2} N_{\phi} |t_N(Q)|^2 \text{Im} [\chi_{R,L,L,R}(-\mathbf{Q}, -\mathbf{Q}, \hbar\omega = eV)] \quad (80)$$

$$-2 \frac{e}{\hbar^2} N_{\phi} |t_N(Q)| \text{Im} [e^{-2ieVt} \chi_{R,L,R,L}(-\mathbf{Q}, +\mathbf{Q}, \hbar\omega = eV)].$$

The response functions in Eq. (80) must be evaluated in a ground state where tunneling and so the parallel magnetic field are absent. Thus, only the response functions of the IL or ISP are relevant in this approach to the tunneling $I - V$. In the liquid state where we have the analytical result given by Eq. (70), the second term in Eq. (80) does not contribute to the tunneling current and we find we the tunneling current of the IL phase for small t_0 ,

$$I_{IL}(t) = \frac{e}{2\hbar} N_{\phi} |t_N(Q)|^2 \pi \sqrt{\frac{A(Q)}{B(Q)}} \delta(eV - \hbar\omega_{IL}(Q)), \quad (81)$$

where $A(Q)$ and $B(Q)$ are given by Eqs. (71) and (72) above and $\omega_{IL}(Q)$ is the Goldstone mode of the IL state whose dispersion is given by Eq. (73). This result is identical to that of Ref. 10, and as pointed out there the peak in the tunneling current can be used to follow the dispersion relation of the Goldstone mode. In the experiment of Spielman et al.², the tunneling amplitude is extremely small and the expression above can be applied provided one introduces a phenomenological broadening due to disorder and thermal fluctuations. This can be achieved rather naturally by substituting a Lorentzian for the delta function in Eq. (81), although the microscopic mechanism leading to this broadening is currently not understood.

Whereas in the IL state, the tunneling current peaks near zero bias only for $B_{\parallel} = 0$, in the ISP the Goldstone mode folds back upon itself, continuously deforming into the phonon mode as the Brillouin zone edge is approached. This means the peak in the tunneling will return to zero bias when B_{\parallel} reaches a value such that $Q = \pm 2n\pi/a$, with $n = 0, 1, 2, 3, \dots$ provided $t_N(Q)$ is not zero. This is illustrated in Fig. 3, which is produced using the first (normal) term in Eq. (80) with a phenomenological broadening parameter δ . This non-monotonic behavior of the tunneling current peak is an unambiguous signature of the ISP that distinguishes it from the IL. In this way one may probe the transition from IL to ISP via measurement of the interlayer tunneling current. Note that the tunneling current vanishes at large B_{\parallel} where $t_N(Q) \rightarrow 0^{18}$.

The perturbative approach used in this section to compute the tunneling current does not capture the full complexity of the phase diagram discussed in Sec. V. To probe the various phase transitions discussed above and the corresponding change in the collective excitations, the response functions must be evaluated in a ground state that includes the parallel magnetic field. That is, the response functions must be evaluated non-perturbatively with respect to the tunneling matrix element t_0 . Work on this problem is currently in progress.

VIII. CONCLUSION

We have shown that, in higher Landau levels ($N > 1$), a parallel magnetic field can induce a complex sequence of phase transitions in the two-dimensional electron gas of a double-quantum-well system. When the separation between the wells or the parallel magnetic field are varied, transitions occur between commensurate and incommensurate liquid or stripe states. Working in the generalized random-phase approximation, we have computed the spectrum of collective excitations of these four ground states showing how the pseudospin-wave mode of the incommensurate liquid phase is modified by the formation of the stripes in each well and by the parallel magnetic field. We believe that the (incommensurate) stripe state could be distinguished from the (incommensurate) liquid state in a tunneling experiment because of the distinctive signature due to the periodicity of the ISP.

IX. ACKNOWLEDGMENTS

This work was supported by a grant from the Natural Sciences and Engineering Research Council of Canada (NSERC) and by NSF Grant No. DMR-0108451.

*

APPENDIX A: DEFINITION OF THE MATRICES F AND D

With

$$S_{\mathbf{q},\mathbf{q}'} = \sin \left[\frac{\mathbf{q} \times \mathbf{q}' l_{\perp}^2}{2} \right] \quad (\text{A1})$$

The matrices F and D of Eq. (64) are given by

$$D_{i,1}(\mathbf{q}, \mathbf{q}') = \hbar \begin{pmatrix} 2iS_{\mathbf{q},\mathbf{q}'} \langle \tilde{\rho}^{R,R}(\mathbf{q} - \mathbf{q}') \rangle & \\ - \langle \tilde{\rho}^{R,L}(\mathbf{q} - \mathbf{q}') \rangle \gamma_{\mathbf{q},\mathbf{q}'} & \\ \langle \tilde{\rho}^{L,R}(\mathbf{q} - \mathbf{q}') \rangle \gamma_{\mathbf{q},\mathbf{q}'}^* & 0 \end{pmatrix}, \quad (\text{A2})$$

$$D_{i,2}(\mathbf{q}, \mathbf{q}') = \hbar \begin{pmatrix} - \langle \tilde{\rho}^{L,R}(\mathbf{q} - \mathbf{q}') \rangle \gamma_{\mathbf{q},\mathbf{q}'} & \\ \langle \tilde{\rho}^{R,R}(\mathbf{q} - \mathbf{q}') \rangle \gamma_{\mathbf{q},\mathbf{q}'}^* - \langle \tilde{\rho}^{L,L}(\mathbf{q} - \mathbf{q}') \rangle \gamma_{\mathbf{q},\mathbf{q}'} & 0 \\ & \\ \langle \tilde{\rho}^{L,R}(\mathbf{q} - \mathbf{q}') \rangle \gamma_{\mathbf{q},\mathbf{q}'}^* & \end{pmatrix}, \quad (\text{A3})$$

$$D_{i,3}(\mathbf{q}, \mathbf{q}') = \hbar \begin{pmatrix} \langle \tilde{\rho}^{R,L}(\mathbf{q} - \mathbf{q}') \rangle \gamma_{\mathbf{q}, \mathbf{q}'}^* \\ 0 \\ \langle \tilde{\rho}^{L,L}(\mathbf{q} - \mathbf{q}') \rangle \gamma_{\mathbf{q}, \mathbf{q}'}^* - \langle \tilde{\rho}^{R,R}(\mathbf{q} - \mathbf{q}') \rangle \gamma_{\mathbf{q}, \mathbf{q}'} \\ - \langle \tilde{\rho}^{R,L}(\mathbf{q} - \mathbf{q}') \rangle \gamma_{\mathbf{q}, \mathbf{q}'} \end{pmatrix}, \quad (\text{A4})$$

$$D_{i,4}(\mathbf{q}, \mathbf{q}') = \hbar \begin{pmatrix} 0 \\ \langle \tilde{\rho}^{R,L}(\mathbf{q} - \mathbf{q}') \rangle \gamma_{\mathbf{q}, \mathbf{q}'}^* \\ - \langle \tilde{\rho}^{L,R}(\mathbf{q} - \mathbf{q}') \rangle \gamma_{\mathbf{q}, \mathbf{q}'} \\ 2iS_{\mathbf{q}, \mathbf{q}'} \langle \tilde{\rho}_m^{L,L}(\mathbf{q} - \mathbf{q}') \rangle \end{pmatrix}, \quad (\text{A5})$$

and (in these definitions, the tunneling $t_N(Q)$ and all matrix elements are in units of $e^2/\kappa\ell$)

$$F_{1,1}(\mathbf{q}, \mathbf{q}') = -2iS_{\mathbf{q}, \mathbf{q}'} \left[[H(\mathbf{q} - \mathbf{q}') - X(\mathbf{q} - \mathbf{q}') - H(\mathbf{q}') + X(\mathbf{q}')] \langle \tilde{\rho}^{R,R}(\mathbf{q} - \mathbf{q}') \rangle \right] \\ - 2iS_{\mathbf{q}, \mathbf{q}'} \tilde{H}(\mathbf{q} - \mathbf{q}') (\gamma^*(\mathbf{q} - \mathbf{q}'))^2 \langle \tilde{\rho}^{L,L}(\mathbf{q} - \mathbf{q}') \rangle, \quad (\text{A6})$$

$$F_{2,1}(\mathbf{q}, \mathbf{q}') = -t_N(Q) \delta_{\mathbf{q}, \mathbf{q}'} - \left[H(\mathbf{q}') - X(\mathbf{q}') + \tilde{X}_-(\mathbf{q} - \mathbf{q}') \right] \langle \tilde{\rho}^{R,L}(\mathbf{q} - \mathbf{q}') \rangle \gamma_{\mathbf{q}, \mathbf{q}'} \\ + \left[\tilde{H}(\mathbf{q}') \gamma^2(\mathbf{q}') \right] \langle \tilde{\rho}^{R,L}(\mathbf{q} - \mathbf{q}') \rangle \gamma_{\mathbf{q}, \mathbf{q}'}^*, \quad (\text{A7})$$

$$F_{3,1}(\mathbf{q}, \mathbf{q}') = t_N(Q) \delta_{\mathbf{q}, \mathbf{q}'} + \left[H(\mathbf{q}') - X(\mathbf{q}') + \tilde{X}_+(\mathbf{q} - \mathbf{q}') \right] \langle \tilde{\rho}^{L,R}(\mathbf{q} - \mathbf{q}') \rangle \gamma_{\mathbf{q}, \mathbf{q}'}^* \\ - \left[\tilde{H}(\mathbf{q}') \gamma^2(\mathbf{q}') \right] \langle \tilde{\rho}^{L,R}(\mathbf{q} - \mathbf{q}') \rangle \gamma_{\mathbf{q}, \mathbf{q}'}^*, \quad (\text{A8})$$

$$F_{4,1}(\mathbf{q}, \mathbf{q}') = 2iS_{\mathbf{q}, \mathbf{q}'} \left[\tilde{H}(\mathbf{q}') \gamma^2(\mathbf{q}') \right] \langle \tilde{\rho}^{L,L}(\mathbf{q} - \mathbf{q}') \rangle, \quad (\text{A9})$$

$$F_{1,2}(\mathbf{q}, \mathbf{q}') = -t_N(Q) \delta_{\mathbf{q}, \mathbf{q}'} - \left[\tilde{X}_+(\mathbf{q} - \mathbf{q}') - \tilde{X}_-(\mathbf{q}') \right] \langle \tilde{\rho}^{L,R}(\mathbf{q} - \mathbf{q}') \rangle \gamma_{\mathbf{q}, \mathbf{q}'}, \quad (\text{A10})$$

$$F_{2,2}(\mathbf{q}, \mathbf{q}') = - \left[H(\mathbf{q} - \mathbf{q}') - X(\mathbf{q} - \mathbf{q}') + \tilde{X}_-(\mathbf{q}') \right] \langle \tilde{\rho}^{R,R}(\mathbf{q} - \mathbf{q}') \rangle \gamma_{\mathbf{q}, \mathbf{q}'}^* \\ + \tilde{H}(\mathbf{q} - \mathbf{q}') (\gamma(\mathbf{q} - \mathbf{q}'))^2 \langle \tilde{\rho}^{R,R}(\mathbf{q} - \mathbf{q}') \rangle \gamma_{\mathbf{q}, \mathbf{q}'} \\ + \left[H(\mathbf{q} - \mathbf{q}') - X(\mathbf{q} - \mathbf{q}') + \tilde{X}_-(\mathbf{q}') \right] \langle \tilde{\rho}^{L,L}(\mathbf{q} - \mathbf{q}') \rangle \gamma_{\mathbf{q}, \mathbf{q}'} \\ - \tilde{H}(\mathbf{q} - \mathbf{q}') (\gamma^*(\mathbf{q} - \mathbf{q}'))^2 \langle \tilde{\rho}^{L,L}(\mathbf{q} - \mathbf{q}') \rangle \gamma_{\mathbf{q}, \mathbf{q}'}^*, \quad (\text{A11})$$

$$F_{3,2}(\mathbf{q}, \mathbf{q}') = 0, \quad (\text{A12})$$

$$F_{4,2}(\mathbf{q}, \mathbf{q}') = t_N(Q) \delta_{\mathbf{q}, \mathbf{q}'} + \left(\frac{e^2}{\kappa l_\perp} \right) \left[\tilde{X}_+(\mathbf{q} - \mathbf{q}') - \tilde{X}_-(\mathbf{q}') \right] \langle \tilde{\rho}^{L,R}(\mathbf{q} - \mathbf{q}') \rangle \gamma_{\mathbf{q}, \mathbf{q}'}^*, \quad (\text{A13})$$

$$F_{1,3}(\mathbf{q}, \mathbf{q}') = t_N(Q) \delta_{\mathbf{q}, \mathbf{q}'} + \left(\frac{e^2}{\kappa l_\perp} \right) \left[\tilde{X}_-(\mathbf{q} - \mathbf{q}') - \tilde{X}_+(\mathbf{q}') \right] \langle \tilde{\rho}^{R,L}(\mathbf{q} - \mathbf{q}') \rangle \gamma_{\mathbf{q}, \mathbf{q}'}^*, \quad (\text{A14})$$

$$F_{2,3}(\mathbf{q}, \mathbf{q}') = 0, \quad (\text{A15})$$

$$\begin{aligned}
F_{3,3}(\mathbf{q}, \mathbf{q}') = & - \left[H(\mathbf{q} - \mathbf{q}') - X(\mathbf{q} - \mathbf{q}') + \tilde{X}_+(\mathbf{q}') \right] \left\langle \tilde{\rho}^{L,L}(\mathbf{q} - \mathbf{q}') \right\rangle \gamma_{\mathbf{q}, \mathbf{q}'}^* \\
& + \tilde{H}(\mathbf{q} - \mathbf{q}') (\gamma^*(\mathbf{q} - \mathbf{q}'))^2 \left\langle \tilde{\rho}^{L,L}(\mathbf{q} - \mathbf{q}') \right\rangle \gamma_{\mathbf{q}, \mathbf{q}'} \\
& + \left[H(\mathbf{q} - \mathbf{q}') - X(\mathbf{q} - \mathbf{q}') + \tilde{X}_+(\mathbf{q}') \right] \left\langle \tilde{\rho}^{R,R}(\mathbf{q} - \mathbf{q}') \right\rangle \gamma_{\mathbf{q}, \mathbf{q}'} \\
& - \tilde{H}(\mathbf{q} - \mathbf{q}') (\gamma(\mathbf{q} - \mathbf{q}'))^2 \left\langle \tilde{\rho}^{R,R}(\mathbf{q} - \mathbf{q}') \right\rangle \gamma_{\mathbf{q}, \mathbf{q}}^*, \tag{A16}
\end{aligned}$$

$$F_{4,3}(\mathbf{q}, \mathbf{q}') = -t_N(Q) \delta_{\mathbf{q}, \mathbf{q}'} - \left[\tilde{X}_-(\mathbf{q} - \mathbf{q}') - \tilde{X}_+(\mathbf{q}') \right] \left\langle \tilde{\rho}^{R,L}(\mathbf{q} - \mathbf{q}') \right\rangle \gamma_{\mathbf{q}, \mathbf{q}'}, \tag{A17}$$

$$F_{1,4}(\mathbf{q}, \mathbf{q}') = 2iS_{\mathbf{q}, \mathbf{q}'} \left\langle \tilde{\rho}^{R,R}(\mathbf{q} - \mathbf{q}') \right\rangle \left[\tilde{H}(\mathbf{q}') (\gamma^*(\mathbf{q}'))^2 \right], \tag{A18}$$

$$\begin{aligned}
F_{2,4}(\mathbf{q}, \mathbf{q}') = & t_N(Q) \delta_{\mathbf{q}, \mathbf{q}'} + \left[\tilde{X}_-(\mathbf{q} - \mathbf{q}') + H(\mathbf{q}') - X(\mathbf{q}') \right] \left\langle \tilde{\rho}^{R,L}(\mathbf{q} - \mathbf{q}') \right\rangle \gamma_{\mathbf{q}, \mathbf{q}'}^* \\
& - \left[\tilde{H}(\mathbf{q}') (\gamma^*(\mathbf{q}'))^2 \right] \left\langle \tilde{\rho}^{R,L}(\mathbf{q} - \mathbf{q}') \right\rangle \gamma_{\mathbf{q}, \mathbf{q}'}, \tag{A19}
\end{aligned}$$

$$\begin{aligned}
F_{3,4}(\mathbf{q}, \mathbf{q}') = & -t_N(Q) \delta_{\mathbf{q}, \mathbf{q}'} - \left[\tilde{X}_+(\mathbf{q} - \mathbf{q}') + H(\mathbf{q}') - X(\mathbf{q}') \right] \left\langle \tilde{\rho}^{L,R}(\mathbf{q} - \mathbf{q}') \right\rangle \gamma_{\mathbf{q}, \mathbf{q}'}, \\
& + \left[\tilde{H}(\mathbf{q}') (\gamma^*(\mathbf{q}'))^2 \right] \left\langle \tilde{\rho}^{L,R}(\mathbf{q} - \mathbf{q}') \right\rangle \gamma_{\mathbf{q}, \mathbf{q}'}^*, \tag{A20}
\end{aligned}$$

$$\begin{aligned}
F_{4,4}(\mathbf{q}, \mathbf{q}') = & -2iS_{\mathbf{q}, \mathbf{q}'} \tilde{H}(\mathbf{q} - \mathbf{q}') \gamma^2(\mathbf{q} - \mathbf{q}') \left\langle \tilde{\rho}^{R,R}(\mathbf{q} - \mathbf{q}') \right\rangle \\
& - 2iS_{\mathbf{q}, \mathbf{q}'} [H(\mathbf{q} - \mathbf{q}') - X(\mathbf{q} - \mathbf{q}') - H(\mathbf{q}') + X(\mathbf{q}')] \left\langle \tilde{\rho}^{L,L}(\mathbf{q} - \mathbf{q}') \right\rangle. \tag{A21}
\end{aligned}$$

¹ H.A. Fertig, Phys. Rev. Lett. **82**, 3693 (1999).

² I. B. Spielman, J. P. Eisenstein, L. N. Pfeiffer, and K. W. West, Phys. Rev. Lett. **84**, 5808 (2000); I. B. Spielman, J. P. Eisenstein, L. N. Pfeiffer, and K. W. West, Phys. Rev. Lett. **87**, 036803 (2001).

³ S. Q. Murphy, J. P. Eisenstein, G. S. Boebinger, L. N. Pfeiffer, and K. W. West, Phys. Rev. Lett. **72**, 728 (1994).

⁴ K. Yang, K. Moon, L. Zheng, A. H. Macdonald, S. M. Girvin, D. Yoshioka, and S. C. Zhang, Phys. Rev. Lett. **72**, 732 (1994).

⁵ See, for example, S. Das Sarma and A. Pinczuk, eds., *Perspectives in Quantum Hall Effects*, (Wiley, New York, 1997) and K. Moon, H. Mori, K. Yang, S. M. Girvin, A. H. Macdonald, L. Zheng, D. Yoshioka, and S. C. Zhang, Phys. Rev. B **51**, 5138 (1995); K. Yang, K. Moon, L. Belkhir, H. Mori, S. M. Girvin, A. H. Macdonald, L. Zheng, and D. Yoshioka, Phys. Rev. B **54**, 11644 (1996).

⁶ L. Brey and H.A. Fertig, Phys. Rev. B **62**, 10268 (2000).

⁷ A.A. Koulakov, M.M. Fogler and B.I. Shklovskii, Phys. Rev. Lett. **76**, 499 (1996); R. Moessner and J.T. Chalker, Phys. Rev. B **54**, 50006 (1996).

⁸ M.P. Lilly, K.B. Cooper, J.P. Eisenstein, L.N. Pfeiffer and K.W. West, Phys. Rev. Lett. **82**, 394 (1999); R.R. Du, D.C. Tsui, H.L. Stormer, L.N. Pfeiffer, K.W. Baldwin and K.W. West, Solid State Comm. **109**, 389 (1999).

⁹ R. Côté and H.A. Fertig, Phys. Rev. B **65**, 85321 (2002).

¹⁰ L. Balents and L. Radzihovsky, Phys. Rev. Lett. **86**, 1825 (2001); Ady Stern, S.M. Girvin, A.H. MacDonald, and Ning Ma, Phys. Rev. Lett. **86**, 1829 (2001).

¹¹ The oscillations of the tunneling amplitude with the parallel magnetic field were also studied by J. Hu and A. H. MacDonald, Phys. Rev. B **46**, 12554 (1992); S. K. Lyo, Mat. Res. Soc. Symp. Proc., vol. 450, 189 (1997).

¹² R. Côté and A.H. MacDonald, Phys. Rev. Lett. **65**, 2662 (1990); Phys. Rev. B **44**, 8759 (1991).

¹³ R. Côté, L. Brey, H. Fertig, and A. H. MacDonald, Phys. Rev. B **51**, 13475 (1995).

¹⁴ E. Demler, D.-W. Wang, S. Das Sarma, and B. I. Halperin, unpublished [cond-mat/0110126 (2001)].

¹⁵ Further evidence of this is found in the static HF solutions, which show a tendency to develop weak oscillations in the in-plane components of the pseudospin just before the transition to the stripe phase, which we interpret as evidence of the SLS instability. These oscillations have only a very small effect on the energy.

¹⁶ For $t_N(\mathbf{Q}) = 0$, $\omega_{CL}(\mathbf{q})$ is gapless. But since the CL is always unstable to the IL in this limit, such gaplessness is never observable in the CL state.

¹⁷ G. D. Mahan, Many-particle physics, 3rd edition, Plenum publishers, New York (2000).

¹⁸ We remark that in the ISP, $\chi_{R,L,R,L}(\mathbf{q}, \mathbf{q}', \omega) = \chi_{R,L,R,L}(\mathbf{k} + \mathbf{G}, \mathbf{k} + \mathbf{G}', \omega)$ where \mathbf{k} is a vector in the first Brillouin zone in the reciprocal lattice and \mathbf{G}, \mathbf{G}' are reciprocal lattice vectors. In computing the tunneling current in Fig. 3, we ignored the second term in Eq. (80) that can contribute to the current only at some discrete values of Q .

¹⁹ L. Zheng and A. H. Macdonald, Phys. Rev. B47, 10619 (1993).